

A Stochastic Observability Test for Discrete-Time Kalman Filters

Vibhor L. Bageshwar¹, Demoz Gebre-Egziabher², William L. Garrard³,
and Tryphon T. Georgiou⁴
University of Minnesota
Minneapolis, MN 55454

Abstract

Stochastic observability refers to the existence of a filter for which the errors of the estimated state mean vector have bounded variance. In this paper, we derive a test to assess the stochastic observability of a Kalman filter implemented for discrete linear time-varying stochastic systems. This test is derived with the assumptions that the system matrices consist of known, deterministic parameters and that there is complete uncertainty in the statistics of the initial state vector. This test can also be used to assess the stochastic observability of extended Kalman filters implemented for nonlinear stochastic systems linearized about the true state vector trajectory. We illustrate the utility of the stochastic observability test using an aided INS. We also provide a counterexample to illustrate that observability is a necessary, but not sufficient, condition for the stochastic observability of a Kalman filter implemented for a system.

Nomenclature

a	acceleration
b	bias
b_0	constant bias null shift
b_1	bias drift rate
\mathcal{C}	$n \times n$ uniform complete controllability grammian

¹ Department of Aerospace Engineering and Mechanics; currently at Honeywell International, Golden Valley, MN, vibhor.bageshwar@honeywell.com, Member AIAA

² Associate Professor, Department of Aerospace Engineering and Mechanics, Member AIAA

³ Professor and Director of the Minnesota Space Grant Consortium, Department of Aerospace Engineering and Mechanics, Fellow AIAA

⁴ Professor, Department of Electrical and Computer Engineering

f	dynamic model
f_b	accelerometer bias
F	continuous-time state error mapping matrix
h	measurement model
H	$p \times n$ measurement matrix
I	identity matrix
K	$n \times p$ Kalman gain matrix
\mathcal{O}	$kp \times n$ observability matrix
$\bar{\mathcal{O}}$	$n \times n$ uniform complete observability grammian
P	$n \times n$ state covariance matrix
Q	$m \times m$ process noise covariance matrix
R	$p \times p$ measurement noise covariance matrix
t	time
T_v	threshold value
U	$n \times n$ unitary matrix
v	$p \times 1$ measurement noise vector
V	$p \times p$ unitary matrix
w	$m \times 1$ process noise vector
x	$n \times 1$ state vector
\bar{x}	$n \times 1$ state mean vector
z	$p \times 1$ measurement vector
Z	measurement vector sequence
$\hat{z}_{k+1 k}$	$p \times 1$ predicted measurement vector
δ	Dirac delta function
δx	$n \times 1$ state error vector
ν	$p \times 1$ innovation vector
τ	correlation time of the process b_1
ω_z	angular velocity about vertical body axis
ω_{bz}	gyro bias
Γ	$n \times m$ process noise mapping matrix
Γ_c	continuous-time process noise mapping matrix
Π	projection operator
Φ	$n \times n$ state mapping matrix

Ψ	heading angle
$n_{(\cdot)}$	additive wide band noise of the measurement of (\cdot)
$p_{(\cdot)}$	position component along (\cdot) direction
$v_{(\cdot)}$	velocity component along (\cdot) direction
$\mathcal{N}(\cdot)$	null space of (\cdot)
$Q_{(\cdot)}$	power spectral density of (\cdot)
$\mathcal{R}(\cdot)$	range space of (\cdot)
$\sigma_{(\cdot)}$	standard deviation of additive wide band noise corresponding to (\cdot)
$\sigma_{\max}(\cdot)$	largest singular value of (\cdot)
$\hat{(\cdot)}$	estimate of (\cdot)
$(\cdot)_a$	accelerometer quantity
$(\cdot)_g$	gyro quantity
$(\cdot)_m$	measurement of (\cdot)
$(\cdot)_x$	component of (\cdot) along \hat{i} body axis
$(\cdot)_y$	component of (\cdot) along \hat{j} body axis
$(\cdot)_E$	component of (\cdot) along E axis
$(\cdot)_N$	component of (\cdot) along N axis
$(\cdot)^\dagger$	pseudoinverse of (\cdot)
$\mathcal{M}_r^{n \times p}$	$n \times p$ matrix with rank r

1 Introduction

In certain applications, the performance objectives of a filter are to compute unbiased, minimum variance estimates of a state mean vector from a set of measurements corrupted by noise. These performance objectives influence the selection of physical components such as sensors, their performance characteristics, and their locations. Furthermore, these performance objectives also influence the selection of sensor measurement models, uncertainty of the dynamic model, the statistics of the initial state vector, and, possibly, the state vector trajectory.

The Kalman filter (KF) is used to estimate the statistics of a state vector whose time evolution is governed by a stochastic system and is intended to be used with Markov processes or sequences with Gaussian distributions. The KF, under various assumptions on the system, can be considered as a model based algorithm that is used to recursively

estimate both the state mean vector and state covariance matrix. The estimated state covariance matrix provides a statistical description of the errors associated with the estimated state mean vector and can be used as a metric to assess whether these estimation errors have bounded variance.

The time evolution of the estimated state covariance matrix is governed by a Riccati equation formulated using the matrices of the stochastic system. This Riccati equation depends on the sensor performance statistics but not the actual sensor measurements. Furthermore, for nonlinear systems, the corresponding Riccati equation is formulated using system models linearized about a state vector trajectory. Therefore, the performance of a KF implemented for a particular stochastic system can be assessed prior to real-time application by evaluating the time evolution of the estimated state covariance matrix.

If the time evolution of all elements of the estimated state covariance matrix are bounded or less than a predefined threshold value, then the filter implemented for the stochastic system is stochastically observable. The threshold value is an application driven design parameter that defines the maximum error of the estimated state mean vector. Conversely, if the time evolution of at least one element of the estimated state covariance matrix is unbounded or greater than a predefined threshold value, then the filter implemented for the stochastic system is stochastically unobservable. The stochastic unobservability of a filter implemented for a system can be caused by several factors including the selection of sensors, system matrices, state vector trajectory, and uncertainty of the initial state vector.

The stochastic observability of a KF implemented for stochastic systems and the convergence and stability of the resulting estimated state mean vector have been the subject of much research. This research can be classified into three general categories. In the first category are studies that consider KFs implemented for linear time-varying (LTV) stochastic systems with system matrices consisting of known, deterministic parameters. In the second category are studies that consider KFs or extended Kalman filters (EKFs) implemented for LTV stochastic systems consisting of unknown, deterministic or stochastic parameters. In the third category are studies that consider EKFs implemented for nonlinear stochastic systems. Studies throughout these categories require certain restrictions on the stochastic system.

In the first category, bounds on the state covariance matrix were derived in terms of the uniform complete observability grammian for systems with no process noise vector

[1]-[4] or in terms of the uniform complete observability grammian and uniform complete controllability grammian by considering the effects of the process noise and measurement noise vectors on the system individually [1], [5], [6]. These bounds are independent of the initial state covariance matrix. The convergence and stability properties of the estimated state mean vector were considered for systems with no measurement noise vector [1], [7], [8], for systems with both process noise and measurement noise vectors [3], and for systems where either the state vector, process noise vector, or measurement noise vector have a non-Gaussian probability density function (pdf) [9].

In the second category, bounds on the state covariance matrix were derived for a general class of systems with restrictions bounding the system matrices [10],[11]. The convergence and stability properties of the estimated state mean vector were considered for a general class of systems with restrictions bounding the system matrices [10]-[12] and for systems designed specifically for certain applications such as parameter estimation [13], [14].

In the third category, the convergence and stability properties of the estimated state mean vector were considered for systems with no noise vectors [15], with system matrices in a specific form [16], and for a general class of systems with restrictions bounding the system matrices and initial state vector statistics [17], [18]. In [17] and [18], stochastic observability of the EKF implemented for the nonlinear stochastic system is a necessary condition for the analysis.

The objective of this paper is to derive a test to assess the stochastic observability of a KF implemented for discrete stochastic systems. More specifically, we consider discrete LTV stochastic systems subject to the following assumptions. First, the system models consist of known, deterministic time-varying parameters. This class of system model includes nonlinear models linearized about the true state vector trajectory. In certain applications, the stochastic observability test can be used to assess the stochastic observability of an EKF implemented for systems with known vehicle maneuvers. Second, the statistics of the initial state vector are completely uncertain.

This paper is organized as follows. In Section 2, we review the general formulation of an EKF. In Section 3, we derive a test to assess the stochastic observability of a KF implemented for a discrete LTV stochastic system. In Section 4, we apply the stochastic observability test to the transfer alignment of an aided inertial navigation system (INS).

2 The Extended Kalman Filter

We consider discrete nonlinear stochastic systems of the form

$$x_{k+1} = f_k(x_k) + \Gamma_k w_k \quad (1a)$$

$$z_k = h_k(x_k) + v_k \quad (1b)$$

We assume that f_k and h_k are C^1 functions and consist of deterministic time-varying parameters. If f_k or h_k are LTV functions, then equations (1a) and (1b) can be modified using

$$f_k(x_k) = \Phi_k x_k \quad (1c)$$

$$h_k(x_k) = H_k x_k \quad (1d)$$

We make the following assumptions regarding the statistics of the stochastic system. First, w_k and v_k are modeled as zero-mean, Gaussian, uncorrelated white sequences with

$$E\{w_k w_k^T\} = Q_k, \quad Q_k \geq 0 \quad (1e)$$

$$E\{v_k v_k^T\} = R_k, \quad R_k > 0 \quad (1f)$$

$$E\{w_i v_j^T\} = 0, \quad \forall i, j \quad (1g)$$

Second, the pdf of the initial state vector is Gaussian with mean \bar{x}_0 and covariance P_0

$$E\{(x_0 - \bar{x}_0)(x_0 - \bar{x}_0)^T\} = P_0 \quad (1h)$$

Third, w_k and v_k are uncorrelated with x_0

$$E\{(x_0 - \bar{x}_0)w_i^T\} = 0 \quad \forall i = 1, \dots, m \quad (1i)$$

$$E\{(x_0 - \bar{x}_0)v_j^T\} = 0 \quad \forall j = 1, \dots, p \quad (1j)$$

The EKF is used to estimate the statistics of the state vector using the following two step procedure at times t_k and t_{k+1} [19], [20]. At time t_k , the state mean vector and state covariance matrix are predicted using the measurement sequence $Z_k = [z_0, \dots, z_k]$

$$\hat{x}_{k+1|k} = f_k(\hat{x}_{k|k}) \quad (2)$$

$$P_{k+1|k} = \Phi_k P_{k|k} \Phi_k^T + \Gamma_k Q_k \Gamma_k^T \quad (3)$$

Equation (2) suggests that the estimated state mean vector is propagated using the dynamic model regardless of its classification as linear or nonlinear. However, if the dynamic model is nonlinear, then the estimated state covariance matrix is propagated using the Jacobian of the dynamic model where

$$\Phi_k = \left. \frac{\partial f_k(x)}{\partial x} \right|_{\hat{x}_{k|k}} \quad (4)$$

At time t_{k+1} , the predicted state mean vector and predicted state covariance matrix are corrected using the measurement vector z_{k+1} and the linear measurement update equations

$$\nu_{k+1} = z_{k+1} - \hat{z}_{k+1|k} \quad (5)$$

$$K_{k+1} = P_{k+1|k} H_{k+1}^T (R_{k+1} + H_{k+1} P_{k+1|k} H_{k+1}^T)^{-1} \quad (6)$$

$$\hat{x}_{k+1|k+1} = \hat{x}_{k+1|k} + K_{k+1} \nu_{k+1} \quad (7)$$

$$P_{k+1|k+1} = P_{k+1|k} - K_{k+1} H_{k+1} P_{k+1|k} \quad (8)$$

If the measurement model is nonlinear, then the correction step is performed using the Jacobian of the measurement model where

$$H_{k+1} = \left. \frac{\partial h_{k+1}(x)}{\partial x} \right|_{\hat{x}_{k+1|k}} \quad (9)$$

In addition to the assumptions previously stated, we make the following additional assumptions for all times t_k . First, f_k and h_k are linearized about the true state vector trajectory. Second, Φ_k , Γ_k , H_k , Q_k , and R_k consist of known, deterministic parameters that are constant throughout the time interval $[t_k, t_{k+1}]$. We will refer to these five matrices as the system matrices throughout the remaining sections of the paper. Third, $(\Phi_k, \Gamma_k \sqrt{Q_k})$ is controllable. Fourth, (Φ_k, H_k) is observable.

The covariance equations of the time and measurement updates can be combined to formulate a discrete time-varying Riccati equation. If equation (8) is substituted into equation (3), then $P_{k+1|k}$ can be rewritten as

$$P_{k+1|k} = \Phi_k P_{k|k-1} \Phi_k^T + \Gamma_k Q_k \Gamma_k^T - \Phi_k K_k H_k P_{k|k-1} \Phi_k^T \quad (10)$$

This Riccati equation relates $P_{k|k-1}$ to $P_{k+1|k}$ without requiring the computation of $P_{k|k}$. If the time updates occur at a faster rate than the measurement updates, then equation

(10) requires suitable modification. If a measurement update occurs every l time updates, then equations (3) and (10) can be rewritten as

$$\begin{aligned} P_{k+l|k} &= \Phi_{k+l,k} P_{k|k} \Phi_{k+l,k}^T + \hat{Q}_k \\ &= \Phi_{k+l,k} P_{k|k-1} \Phi_{k+l,k}^T + \hat{Q}_k - \Phi_{k+l,k} K_k H_k P_{k|k-1} \Phi_{k+l,k}^T \end{aligned} \quad (11)$$

where

$$\hat{Q}_k = \sum_{i=k}^{k+l-1} \Phi_{k+l-1,i+1} \Gamma_i Q_i \Gamma_i^T \Phi_{k+l-1,i+1}^T,$$

$\Phi_{k+l,k} = \Phi_{k+l} \cdots \Phi_k$, and $\Phi_{k+l,k}^T = \Phi_k^T \cdots \Phi_{k+l}^T$. The Riccati equation, equation (10) or more generally equation (12), governs the time evolution of the estimated state covariance matrix. We simplify the notation $P_{k+1|k}$ to P_{k+1} throughout the remaining sections of the paper.

3 Observability Tests

Observability is a property of combinations of the system matrices as specified in equation (1). The objectives of this section are to define observability and stochastic observability, to identify the relationship between these two types of observability and their effect on KF performance, and to derive a test to assess the stochastic observability of a KF implemented for the system, equation (1).

3.1 Observability

The observability of LTV or linearized systems with no process or measurement noise vectors can be defined as follows [19], [20].

Definition 1: A LTV or linearized system with no process or measurement noise vectors is observable at time t_N if the state vector at time t_N , x_N , can be determined from operations on the measurement sequence $Z_N = [z_0, \dots, z_N]$ where $t_N > t_0$ and $t_N < \infty$.

One test to assess the observability of a system involves evaluating the rank of the observability grammian, $\mathcal{O}_N^T \mathcal{O}_N$, where [19], [20]

$$\mathcal{O}_N^T \mathcal{O}_N = H_0^T H_0 + \sum_{k=1}^N \Phi_{k-1,0}^T H_k^T H_k \Phi_{k-1,0} \quad (12)$$

If $\mathcal{O}_N^T \mathcal{O}_N$ has full rank, then the system is observable. This test is based on evaluating the rank of a $n \times n$ matrix whose dimensions depend only on the dimensions of the state vector and not on the dimensions of the measurement vector or number of measurements.

An observable system ensures that all states of the state mean vector can be influenced by the measurement vector. The test for observability does not incorporate the noise covariance matrices, Q_k and R_k , or the statistics of the initial state vector, P_0 . However, the Riccati equation that governs the time evolution of the state covariance matrix depends on all five system matrices and the statistics of the initial state vector. Regardless of whether the Φ and H matrices of equation (1) satisfy the observability condition, Q_k , R_k , or P_0 could cause the state covariance matrix to become unbounded or exceed a predefined threshold value. Therefore, observability is a necessary, but not sufficient, condition to ensure that the errors of the estimated state mean vector have bounded variance.

3.2 Stochastic Observability

The stochastic observability of the system as specified in equation (1) can be defined as follows [21].

Definition 2: The system specified in equation (1) is stochastically observable if there exists a finite time t_N such that the state covariance matrix is bounded or less than a predefined threshold value, T_v , in the sense that

$$\sigma_{\max}(P_k) < T_v \quad t_k \geq t_N \quad (13)$$

where $T_v, t_N < \infty$ and $\sigma_{\max}(\cdot)$ refers to the largest singular value of the matrix (\cdot) .

Definition 2 is slightly modified from the definition given in [21] in three ways. First, we have used the maximum singular value of P_k as the measure of whether the estimated state covariance matrix has converged to a finite limit. Second, we have referred to this limit as the threshold value. Third, we have added the condition that once $\sigma_{\max}(P_k)$ is less than the threshold value for $t_k = t_N$, $\sigma_{\max}(P_k)$ must also be less than the threshold value for $t_k > t_N$.

A test to assess the stochastic observability of a KF implemented for discrete LTV systems subject to complete uncertainty of the statistics of the initial state vector is developed in the following three lemmas. The first two lemmas reorganize the Riccati equation

into terms that have similar dependence on P_0 . The third lemma provides conditions for which the state covariance matrix is bounded or less than a predefined threshold value. We first define notation used for projection operators, or projectors, required in these lemmas. We denote $\Pi_{\mathcal{R}(\Theta)}$ as the projector onto the range space of the matrix Θ [22]

$$\Pi_{\mathcal{R}(\Theta)} = \Theta(\Theta^T\Theta)^\dagger\Theta^T \quad (14)$$

We denote $\Pi_{\mathcal{N}(\Theta^T)}$ as the projector onto the orthogonal complement of the range space of Θ [22]

$$\Pi_{\mathcal{N}(\Theta^T)} = I - \Pi_{\mathcal{R}(\Theta)} \quad (15)$$

Lemma 1: Consider the system specified in equation (1) and assume that the initial state covariance matrix is selected as

$$P_0 = \alpha I \quad \alpha \in \mathfrak{R}, \alpha > 0 \quad (16)$$

then the Riccati equation, equation (10), can be rewritten as

$$P_{k+1} = \alpha\Lambda_{k+1} + \bar{Q}_{k+1} + \Delta_{k+1}(\alpha^{-1}) \quad (17)$$

where

$$\Lambda_1 = \Phi_0\Omega_0\Omega_0^T\Phi_0^T \quad (17a)$$

$$\Lambda_{k+1} = \Phi_{k,0}\Omega_{0,k}\Omega_{0,k}^T\Phi_{k,0}^T \quad k > 0 \quad (17b)$$

$$\bar{Q}_1 = \Gamma_0Q_0\Gamma_0^T + \Phi_0\Theta_0((\Theta_0^T\Theta_0)^\dagger)^2\Theta_0^T\Phi_0^T \quad (17c)$$

$$\bar{Q}_{k+1} = \bar{Q}_{k+1}(\Lambda_k, \bar{Q}_k, \Phi_k, \Gamma_k, Q_k, H_k, R_k) \quad k > 0 \quad (17d)$$

$$\Delta_1(\alpha^{-1}) = -\Phi_0[\alpha^{-1}\Theta_0((\Theta_0^T\Theta_0)^\dagger)^4\Theta_0^T + \dots]\Phi_0^T \quad (17e)$$

$$\Delta_{k+1}(\alpha^{-1}) = \Delta_{k+1}(\alpha^{-1}, \Lambda_k, \bar{Q}_k, \Delta_k, \Phi_k, \Gamma_k, Q_k, H_k, R_k) \quad k > 0 \quad (17f)$$

and

$$\Pi_{\mathcal{N}(\Theta_k^T)} = \Omega_k\Omega_k^T \quad k \geq 0$$

$$\Omega_{0,k} = \Omega_0 \cdots \Omega_k$$

$$\Upsilon_0^T\Upsilon_0 = R_0$$

$$\Upsilon_k^T\Upsilon_k = R_k + H_k\bar{Q}_kH_k^T \quad k > 0$$

$$\Theta_0 = H_0^T\Upsilon_0^{-1}$$

$$\Theta_k = \Omega_{0,k-1}^T\Phi_{k-1,0}^T H_k^T\Upsilon_k^{-1} \quad k > 0$$

The matrices \bar{Q}_{k+1} and $\Delta_{k+1}(\alpha^{-1})$ are defined in equation (A.36). The matrix Ω_k has the same rank as $\Pi_{\mathcal{N}(\Theta_k^T)}$.

Proof: The proof is given in Appendix A.

Lemma 2: Under the conditions of Lemma 1, if the following condition is satisfied

$$\sigma_{\max}(\Lambda_j) = 0 \quad (18)$$

where Λ is defined in equation (17) and $t_j < \infty$, then $\sigma_{\max}(\Lambda_{k+1}) = 0$ for all $t_k \geq t_j$ and the Riccati equation, equation (10), can be rewritten as

$$P_{k+1} = \bar{Q}_{k+1} + \Delta_{k+1}(\alpha^{-1}) \quad t_k \geq t_j \quad (19)$$

where

$$\bar{Q}_{k+1} = \bar{Q}_{k+1}(\bar{Q}_k, \Phi_k, \Gamma_k, Q_k, H_k, R_k) \quad k \geq j > 0 \quad (19a)$$

$$\Delta_{k+1}(\alpha^{-1}) = \Delta_{k+1}(\alpha^{-1}, \bar{Q}_k, \Delta_k, \Phi_k, \Gamma_k, Q_k, H_k, R_k) \quad k \geq j > 0 \quad (19b)$$

The matrices \bar{Q}_{k+1} and $\Delta_{k+1}(\alpha^{-1})$ are defined in equation (A.42).

Proof: Lemma 1 shows that at each time t_k , the Riccati equation can be rewritten as $P_{k+1} = \alpha\Lambda_{k+1} + \bar{Q}_{k+1} + \Delta_{k+1}(\alpha^{-1})$. If condition (18) holds, then $P_{k+1} = \bar{Q}_{k+1} + \Delta_{k+1}(\alpha^{-1})$. The matrices \bar{Q}_{k+1} and Δ_{k+1} are formulated in Appendix A.

Lemma 3: Under the conditions of Lemma 1, if the following two conditions are satisfied

$$\sigma_{\max}(\Lambda_j) = 0 \quad t_j < \infty \quad (18)$$

$$\sigma_{\max}(\bar{Q}_{k+1}) < T_v \quad T_v < \infty, t_k \geq t_j \quad (20)$$

where Λ and \bar{Q} are defined in equations (17) and (19), respectively, then as the scalar $\alpha \rightarrow \infty$, the KF implemented for the system is stochastically observable.

Proof: Lemma 1 shows that at each time t_k , the Riccati equation can be rewritten as $P_{k+1} = \alpha\Lambda_{k+1} + \bar{Q}_{k+1} + \Delta_{k+1}(\alpha^{-1})$. Lemma 2 shows that if condition (18) holds, then $P_{k+1} = \bar{Q}_{k+1} + \Delta_{k+1}(\alpha^{-1})$, equation (19). If we take the limit of equation (19) as $\alpha \rightarrow \infty$, then

$$\begin{aligned} \lim_{\alpha \rightarrow \infty} P_{k+1} &= \lim_{\alpha \rightarrow \infty} (\bar{Q}_{k+1} + \Delta_{k+1}(\alpha^{-1})) \\ &= \bar{Q}_{k+1} + \lim_{\alpha \rightarrow \infty} \Delta_{k+1}(\alpha^{-1}) \\ &= \bar{Q}_{k+1} \end{aligned} \quad (21)$$

If condition (20) holds, then

$$\sigma_{\max}(\bar{Q}_{k+1}) = \sigma_{\max}\left(\lim_{\alpha \rightarrow \infty} P_{k+1}\right) < T_v \quad (22)$$

There are several observations that can be made regarding Lemmas 1-3.

1) The assumptions $P_0 = \alpha I$ and $\alpha \rightarrow \infty$ imply that the KF is initialized with no *a priori* information available about the statistics of the initial state vector.

2) The matrices Λ_{k+1} and \bar{Q}_{k+1} are formulated from terms that do not include the scalar α or the matrix $\Delta_k(\alpha^{-1})$. Therefore, the assumption $\alpha \rightarrow \infty$ plays no role either in the formulation of these matrices or the conditions $\sigma_{\max}(\Lambda_j) = 0$ and $\sigma_{\max}(\bar{Q}_{k+1}) < T_v$.

3) The matrix \bar{Q}_{k+1} , formulated using either Lemmas 1 or 2, includes both positive and negative terms. Therefore, $\sigma_{\max}(\bar{Q}_{k+1})$ does not necessarily increase at each time step.

4) The matrix $\Delta_{k+1}(\alpha^{-1})$ consists of terms that have α^{-1} as a coefficient. Therefore, the assumption $\alpha \rightarrow \infty$ implies that $\Delta_{k+1}(\alpha^{-1}) = 0$ and that $\Delta_{k+1}(\alpha^{-1})$ consists of infinitesimal terms whose contributions to the state covariance matrix can be neglected.

5) The condition $\sigma_{\max}(\Lambda_j) = 0$ requires the modes of the matrices Φ_0, \dots, Φ_j to be orthogonal to the modes of the projectors $\Pi_{\mathcal{N}(\Theta_0^T)}, \dots, \Pi_{\mathcal{N}(\Theta_j^T)}$. This condition and the assumptions $P_0 = \alpha I$ and $\alpha \rightarrow \infty$ imply that the state covariance matrix is not a function of α and, thus, the initial state vector statistics for all times $t_k, t_k \geq t_j$.

6) The condition $\sigma_{\max}(\bar{Q}_{k+1}) < T_v$ implies that increases to P_{k+1} due to contributions from Φ_k, Γ_k, Q_k , and \bar{Q}_k are offset by decreases to P_{k+1} due to contributions from Φ_k, H_k, R_k , and \bar{Q}_k . Therefore, if this condition fails, then alternative sensors, system matrices, or state vector trajectories should be used when formulating the stochastic system.

7) The condition $\sigma_{\max}(\Lambda_j) = 0$ must be satisfied prior to checking the condition $\sigma_{\max}(\bar{Q}_{k+1}) < T_v$.

The stochastic observability test developed in Lemmas 1-3 is summarized in Figure 1. This test is based on evaluating the singular values of two $n \times n$ matrices whose dimensions depend only on the dimensions of the state vector. If the conditions of the test are satisfied, then the KF implemented for the system specified in equation (1) will be stochastically observable for any P_0 . Therefore, if a KF implemented for a system is stochastically observable for a large P_0 and the conditions of the stochastic observability test are satisfied,

then the system will remain stochastically observable even if P_0 is modified. In other words, this stochastic observability test can be used to assess whether a large P_0 will destabilize a KF implemented for the system.

However, this test is conservative because it provides conditions for stochastic observability for the worst case P_0 . For example, consider a filter implemented for a system that is stochastically observable for $\sigma_{\max}(P_0) < \infty$ but is stochastically unobservable for $P_0 = \alpha I$, $\alpha \rightarrow \infty$. If the stochastic observability test is applied to this example, then one of the two conditions (18) or (20) will fail and the test will indicate that the KF implemented for the system is stochastically unobservable. Therefore, this test provides sufficient, but not necessary, conditions to assess the stochastic observability of a KF implemented for a system.

In [1], [5]-[8], and [11], bounds on the state covariance matrix for LTV stochastic systems were derived and are of the form

$$(\bar{\mathcal{O}}_{k,k-l} + \mathcal{C}_{k,k-l}^{-1})^{-1} \leq P_k \leq \bar{\mathcal{O}}_{k,k-l}^{-1} + \mathcal{C}_{k,k-l} \quad (23)$$

where $\bar{\mathcal{O}}_{k,k-l} = \sum_{i=k-l}^{k-1} \Phi_{i,k}^T H_i^T R_i^{-1} H_i \Phi_{i,k}$ and $\mathcal{C}_{k,k-l} = \sum_{i=k-l}^{k-1} \Phi_{k,i+1}^T \Gamma_i Q_i \Gamma_i^T \Phi_{k,i+1}$. These bounds were derived by using the information form of the KF and the LTV system in two forms. First, bounds on P_k were derived using a system with a process noise vector but with no measurement noise vector to derive \mathcal{C} . Second, bounds on P_k were derived using a system with a measurement noise vector but with no process noise vector to derive $\bar{\mathcal{O}}$. These grammians were then combined using the superposition principle to derive equation (23).

The test given in equation (23) can be used to perform an yes/no assessment of the stochastic observability of a KF implemented for a stochastic system. The stochastic observability test derived in this paper requires more matrix multiplications than equation (23), however, this test provides an exact expression for P_{k+1} and allows the filter designer to identify the causes of a system's stochastic unobservability. We note that the expressions for \bar{Q}_{k+1} , equations (17) and (19), include \mathcal{C} exactly and $\bar{\mathcal{O}}$ in a slightly modified form.

4 Application of the Observability Tests

In this section, we demonstrate the utility of the stochastic observability test developed in Section 3 by analyzing the observability of a problem of significant current research

interest: the transfer alignment of an aided INS [23]. In this application, known vehicle maneuvers are used as inputs to excite particular modes of the INS or, more specifically, to make the heading angle observable. Therefore, filter performance can be evaluated for various vehicle maneuvers prior to real-time filter implementation. We note that the stochastic system is nonlinear for this application, however, the linearization of the system's nonlinear models is about a known state vector trajectory. Therefore, the resulting linearized system is a discrete LTV system consisting of known, deterministic parameters.

The observability analysis of this problem is typically conducted using a three-step procedure. First, a vehicle maneuver is selected. Second, various forms of the observability grammian are evaluated for the resulting stochastic system. Third, the EKF performance is evaluated for the resulting system [24]-[26]. This approach is inevitably limited to specific vehicle maneuvers and not applicable for arbitrary vehicle maneuvers. We, therefore, select two vehicle maneuvers, apply both the observability and stochastic observability tests to the resulting systems, and assess the performance of both tests. The EKF simulations and application of the observability tests were performed using Matlab.

4.1 The Aided INS

Kinematic state refers to a vehicle's position, velocity, and attitude. The kinematic state of a vehicle can be defined by specifying the relative position, velocity, and orientation of two reference frames. The two reference frames typically used are a vehicle fixed body frame and a navigation frame with known orientation. In this application, we select a North-East-Down (NED) frame as the navigation frame. An INS is used to estimate the kinematic state of the vehicle or, more specifically, to estimate the position vector, velocity vector, and orientation of the body frame relative to the navigation frame.

An INS refers to a set of sensors that continuously measure the vehicle's acceleration and angular velocity vectors, and the mathematical operations required to compute estimates of the vehicle's kinematic state. The acceleration vector is measured using accelerometers fixed to the vehicle and aligned with the axes of the vehicle's body frame. Integrating these measurements once yields the vehicle's velocity vector resolved in the vehicle's body frame. Integrating these measurements twice yields the vehicle's position vector resolved in the vehicle's body frame. However, a meaningful kinetic state requires the vehicle's position and velocity vectors to be resolved in the navigation frame. The

angular velocity vector is measured using rate gyros, or simply gyros, fixed to the vehicle and aligned with the axes of the vehicle's body frame. Integrating these measurements once yields the orientation of the vehicle's body frame relative to the navigation frame so that the measured acceleration vector can be resolved in the navigation frame.

One component of an INS is to integrate the accelerometer and gyro measurements. Therefore, certain components of the accelerometer and gyro measurement errors, such as bias, result in potentially unbounded errors in the INS based estimates of the vehicle's kinematic state. These kinematic state errors can be bounded using measurements from aiding sensors such as GPS sensors or magnetometers. The measurements from aiding sensors are independent of the INS measurements and can be used to periodically estimate the accelerometer and gyro biases and reset the INS based estimates of the vehicle's kinematic state. An aided INS fuses measurements from the INS and aiding sensors to compute bounded estimates of the vehicle's kinematic state.

We consider a constrained, or two-dimensional, form of the aided INS, Figure 2. In this application, a vehicle, equipped with an aided INS, travels in the N-E plane of an NED frame. This INS is mechanized using two accelerometers and a gyro. The accelerometers are fixed to the vehicle's body \hat{i}_b and \hat{j}_b axes and measure the specific force vector in the N-E plane. The gyro measures the vehicle's rotation rate about its vertical body axis. Three system architectures will be used to aid the INS. The first system architecture provides measurements of the vehicle's position and velocity vectors, and heading angle and will be referred to as a PVH aided INS. The second system architecture provides measurements of the vehicle's position and velocity vectors and will be referred to as a PV aided INS. The third system architecture provides measurements of the vehicle's position vector and will be referred to as a P aided INS.

An EKF can be used to fuse the sensor measurements from the INS and aiding systems and compute estimates of the vehicle's kinematic state. The aiding sensors of the PV and P aided INS architectures do not directly measure the vehicle's heading angle. However, the vehicle's heading angle can be indirectly measured by the aiding sensors if these modes are excited by persistent, or periodic, acceleration. Therefore, vehicle maneuvers can be used as a component of the aided INS and bound the errors of the INS based estimates of the vehicle's kinematic state.

The performance of the EKF implemented for the three aided INS architectures is evaluated using two scenarios. In the first scenario, or scenario A, the vehicle is traveling

East at a velocity of 30 m/s . At time $t_0 = 0\text{ s}$, the vehicle begins to turn North at a constant heading angle rate of $-0.237^\circ/\text{s}$ while maintaining a constant speed of 30 m/s . In the second scenario, or scenario B, the vehicle travels East as a constant speed of 30 m/s . This two-dimensional sensor fusion problem will allow us to implement the observability tests and avoid details of the three-dimensional aided INS that are not relevant to the current discussion.

4.2 Aided INS Sensor Models

The aided INS sensor measurements for the three architectures and two scenarios were simulated as follows. The accelerometer and gyro measurements were generated using the models

$$a_{mx}(t) = a_x(t) + f_{bx}(t) + n_{ax}(t) \quad (24a)$$

$$a_{my}(t) = a_y(t) + f_{by}(t) + n_{ay}(t) \quad (24b)$$

$$\omega_{mz}(t) = \omega_z(t) + \omega_{bz}(t) + n_g(t) \quad (25)$$

A general model for either the accelerometer or gyro bias is [27]

$$b(t) = b_0 + b_1(t) \quad (26)$$

The bias drift rate can be modeled as a zero-mean, Gaussian, exponentially correlated process where

$$\dot{b}_1(t) = -\frac{1}{\tau}b_1(t) + n_b(t) \quad (27)$$

$$E\{b_1(t)b_1(\tau)\} = \sigma_{b_1}^2 \exp(t - \tau) \quad (27a)$$

$$Q_{b_1} = \frac{2\sigma_{b_1}^2}{\tau} \quad (27b)$$

The noise term n_b can be modeled as a zero-mean, Gaussian, white noise process where

$$E\{n_b(t)n_b(\tau)\} = \sigma_b^2 \delta(t - \tau) \quad (27c)$$

We will select $\sigma_{b_1} = \sigma_b$ in this application.

The wide band noise terms n_{ax} , n_{ay} , and n_g are modeled as zero-mean, Gaussian, white noise processes where

$$E\{n_{ax}(t)n_{ax}(\tau)\} = \sigma_{ax}^2 \delta(t - \tau), \quad (28)$$

$$E\{n_{ay}(t)n_{ay}(\tau)\} = \sigma_{ay}^2 \delta(t - \tau), \quad (29)$$

$$E\{n_g(t)n_g(\tau)\} = \sigma_g^2 \delta(t - \tau) \quad (30)$$

It should be noted that the measurement noise has a higher frequency content than the bias drift rate.

The aiding system measurements were generated using the models

$$p_{mN}(t) = p_N(t) + n_{pN}(t) \quad (31)$$

$$p_{mE}(t) = p_E(t) + n_{pE}(t) \quad (32)$$

$$v_{mN}(t) = v_N(t) + n_{vN}(t) \quad (33)$$

$$v_{mE}(t) = v_E(t) + n_{vE}(t) \quad (34)$$

$$\Psi_m(t) = \Psi(t) + n_\Psi(t) \quad (35)$$

The wide band noise terms n_{pN} , n_{pE} , n_{vN} , n_{vE} , and n_Ψ are modeled as zero-mean, Gaussian, white noise processes where

$$E\{n_{pN}(t)n_{pN}(\tau)\} = \sigma_{pN}^2 \delta(t - \tau) \quad (36)$$

$$E\{n_{pE}(t)n_{pE}(\tau)\} = \sigma_{pE}^2 \delta(t - \tau) \quad (37)$$

$$E\{n_{vN}(t)n_{vN}(\tau)\} = \sigma_{vN}^2 \delta(t - \tau) \quad (38)$$

$$E\{n_{vE}(t)n_{vE}(\tau)\} = \sigma_{vE}^2 \delta(t - \tau) \quad (39)$$

$$E\{n_\Psi(t)n_\Psi(\tau)\} = \sigma_\Psi^2 \delta(t - \tau) \quad (40)$$

The statistics of the aided INS sensors are summarized in Table 1.

4.3 Aided INS System Models

The dynamic model of the stochastic system corresponding to all three aided INS architectures is formulated using the equations

$$\dot{p}_N(t) = v_N(t) \quad (41)$$

$$\dot{p}_E(t) = v_E(t) \quad (42)$$

$$\dot{v}_N(t) = a_N(t) \quad (43)$$

$$\dot{v}_E(t) = a_E(t) \quad (44)$$

$$\dot{\Psi}(t) = \omega_z(t) \quad (45)$$

$$\dot{\hat{f}}_{bx}(t) = 0 \quad (46)$$

$$\dot{\hat{f}}_{by}(t) = 0 \quad (47)$$

$$\dot{\hat{\omega}}_{bz}(t) = 0 \quad (48)$$

where the state vector for all three architectures is

$$x(t) = [p_N(t) \quad p_E(t) \quad v_N(t) \quad v_E(t) \quad \Psi(t) \quad f_{bx}(t) \quad f_{by}(t) \quad \omega_{bz}(t)]^T \quad (49)$$

The accelerometer measurements are resolved in the NED frame using the two-dimensional direction cosine matrix

$$\begin{bmatrix} a_N(t) \\ a_E(t) \end{bmatrix} = \begin{bmatrix} \cos \Psi(t) & -\sin \Psi(t) \\ \sin \Psi(t) & \cos \Psi(t) \end{bmatrix} \begin{bmatrix} a_x(t) \\ a_y(t) \end{bmatrix} \quad (50)$$

The equations used to formulate and propagate the state covariance matrix are based on the state error vector equations which can be summarized as

$$\delta x(t) = x(t) - \hat{x}(t) \quad (51)$$

$$= [\delta p_N(t) \quad \delta p_E(t) \quad \delta v_N(t) \quad \delta v_E(t) \quad \delta \Psi(t) \quad \delta f_{bx}(t) \quad \delta f_{by}(t) \quad \delta \omega_{bz}(t)]^T$$

$$\delta \dot{x}(t) = F(t)\delta x(t) + \Gamma_c(t)w(t) \quad (52)$$

$$F(t) = \begin{bmatrix} 0 & 0 & 1 & 0 & 0 & 0 & 0 & 0 \\ 0 & 0 & 0 & 1 & 0 & 0 & 0 & 0 \\ 0 & 0 & 0 & 0 & F(3,5) & -\cos \hat{\Psi} & \sin \hat{\Psi} & 0 \\ 0 & 0 & 0 & 0 & F(4,5) & -\sin \hat{\Psi} & -\cos \hat{\Psi} & 0 \\ 0 & 0 & 0 & 0 & 0 & 0 & 0 & -1 \\ 0 & 0 & 0 & 0 & 0 & -1/\tau_{ax} & 0 & 0 \\ 0 & 0 & 0 & 0 & 0 & 0 & -1/\tau_{ay} & 0 \\ 0 & 0 & 0 & 0 & 0 & 0 & 0 & -1/\tau_g \end{bmatrix}$$

$$\begin{aligned}
F(3, 5) &= -(a_{mx} - \hat{f}_{bx}) \sin \hat{\Psi} - (a_{my} - \hat{f}_{by}) \cos \hat{\Psi} \\
F(4, 5) &= (a_{mx} - \hat{f}_{bx}) \cos \hat{\Psi} - (a_{my} - \hat{f}_{by}) \sin \hat{\Psi}
\end{aligned}$$

The process noise vector is selected as

$$\begin{aligned}
w(t) &= [n_{ax}(t) \quad n_{ay}(t) \quad n_g(t) \quad n_{abx}(t) \quad n_{aby}(t) \quad n_{gb}(t)]^T \\
\Gamma_c(t) &= \begin{bmatrix} 0 & 0 & 0 & 0 & 0 & 0 \\ 0 & 0 & 0 & 0 & 0 & 0 \\ -\cos \hat{\Psi} & \sin \hat{\Psi} & 0 & 0 & 0 & 0 \\ -\sin \hat{\Psi} & -\cos \hat{\Psi} & 0 & 0 & 0 & 0 \\ 0 & 0 & -1 & 0 & 0 & 0 \\ 0 & 0 & 0 & 1 & 0 & 0 \\ 0 & 0 & 0 & 0 & 1 & 0 \\ 0 & 0 & 0 & 0 & 0 & 1 \end{bmatrix}
\end{aligned} \tag{53}$$

The process noise vector shows that the uncertainty of the dynamic model is due to INS sensor error components. The power spectral density matrix of the process noise vector is selected as

$$Q_w = \text{diag} \left[\sigma_{ax}^2, \sigma_{ay}^2, \sigma_g^2, \frac{2\sigma_{ab1x}^2}{\tau_a}, \frac{2\sigma_{ab1y}^2}{\tau_a}, \frac{2\sigma_{gb1}^2}{\tau_g} \right] \tag{53a}$$

The measurement model used to correct the predicted state mean vector and state covariance matrix is selected as

$$z_k = H_k \hat{x}_{k|k-1} + v_k \tag{54}$$

where for the PVH aiding system

$$H_{PVH,k} = [I_5 \quad 0_{5 \times 3}] \tag{55a}$$

$$R_{PVH,k} = \text{diag} [\sigma_{pN}^2, \sigma_{pE}^2, \sigma_{vN}^2, \sigma_{vE}^2, \sigma_{\Psi}^2], \tag{55b}$$

for the PV aiding system

$$H_{PV,k} = [I_4 \quad 0_{4 \times 4}] \tag{56a}$$

$$R_{PV,k} = \text{diag} [\sigma_{pN}^2, \sigma_{pE}^2, \sigma_{vN}^2, \sigma_{vE}^2], \tag{56b}$$

and for the P aiding system

$$H_{P,k} = [I_2 \quad 0_{2 \times 6}] \tag{57a}$$

$$R_{P,k} = \text{diag} [\sigma_{pN}^2, \sigma_{pE}^2] \tag{57b}$$

The general design of the EKF for the aided INS architectures is shown in Figure 3.

4.4 EKF Performance

The EKFs for the aided INS architectures were simulated for both scenarios using discretized versions of equations (41)-(53) [20]

$$\Phi_k = \exp[F(t_{k+1} - t_k)] \quad (58)$$

$$\Gamma_k = I_8 \quad (59)$$

$$Q_k = \int_{t_k}^{t_{k+1}} \Phi(t_{k+1}, \tau) \Gamma_c(\tau) Q_w(\tau) \Gamma_c^T(\tau) \Phi(t_{k+1}, \tau)^T d\tau \quad (60)$$

The statistics of the initial state vector for all simulations were selected as

$$\bar{x}_0 = [0 \text{ m} \quad 0 \text{ m} \quad 0 \text{ m/s} \quad 30 \text{ m/s} \quad 90^\circ \quad 0 \text{ m/s}^2 \quad 0 \text{ m/s}^2 \quad 0^\circ/\text{s}]^T \quad (61)$$

$$P_0 = 100 \times \text{diag}[0.1^2, 0.1^2, 0.01^2, 0.01^2, 0.25^2, (0.001g)^2, (0.002g)^2, 0.05^2] \quad (62)$$

The time and measurement update rates for all simulations were 10 Hz . We note that the linearization of the nonlinear models was performed using the true state vector trajectory.

Figures 4 and 5 show the EKF performance for scenario A with the PVH aided INS architecture. Figures 6 and 7 show the EKF performance for scenario A with the PV aiding INS architecture. Figures 8 and 9 show the EKF performance for scenario B with the P aided INS architecture. In Figures 4, 6, and 8, the estimated state mean vector is represented by solid lines whereas the true state vector is represented by dashed lines. In Figures 5, 7, and 9, the state error vector is represented by solid lines whereas the $1 - \sigma$ estimation error bands are represented by dashed lines.

Figures 4 and 5 show that the EKF computed unbiased estimates of the vehicle's kinematic state. Furthermore, these figures show that the estimates of the vehicle's kinematic state converged to within their $1 - \sigma$ estimation error bands. The estimates of the accelerometer and gyro null shifts show the effect of both the correlated and uncorrelated bias components. The estimates of the accelerometer null shifts remained within their $1 - \sigma$ estimation error bands. However, the estimates of the gyro null shift required 100 s to converge within its $1 - \sigma$ estimation error bands. It should be noted that all $1 - \sigma$ estimation error bands were bounded. These figures show that the PVH aided INS architecture can

estimate the vehicle’s kinematic state as well as the accelerometer and gyro null shifts for the vehicle maneuver in scenario A.

Figures 6 and 7 show that the EKF computed a biased estimate of the gyro null shift of approximately $0.09^\circ/s$. The biased estimate of the gyro null shift resulted in an estimation error of the vehicle’s heading angle. The EKF computed unbiased estimates of the four remaining vehicle kinematic states. The estimates of the accelerometer null shifts show the effect of both the correlated and uncorrelated bias components. Furthermore, these figures show that the estimates of the vehicle’s position and velocity vectors as well as the accelerometer null shifts converged to within their $1 - \sigma$ estimation error bands. It should be noted that the $1 - \sigma$ estimation error bands for the heading angle diverged whereas the $1 - \sigma$ estimation error bands for the seven remaining states were bounded. These figures show that the vehicle’s maneuver in scenario A was insufficient to enable the PV aided INS architecture to estimate the vehicle’s heading angle and gyro null shift.

Figures 8 and 9 show that the EKF computed a biased estimate of the gyro null shift of $0.5^\circ/s$ and, thus, the EKF was completely unable to estimate the gyro null shift. The biased estimate of the gyro null shift results in a linear estimation error of the vehicle’s heading angle. The EKF computed unbiased estimates of the four remaining vehicle kinematic states. The estimates of the accelerometer null shifts showed the effect of both the correlated and uncorrelated bias components. Furthermore, these figures show that the estimates of the vehicle’s position and velocity vectors as well as the accelerometer null shifts converged to within their $1 - \sigma$ estimation error bands within $50 s$. It should be noted that the $1 - \sigma$ estimation error bands for the heading angle diverged whereas the $1 - \sigma$ estimation error bands for the seven remaining states were bounded. These figures show that the vehicle’s maneuver in scenario B was insufficient to enable the P aided INS architecture to estimate the vehicle’s heading angle and the gyro bias.

4.5 Observability Tests

The observability of the EKFs implemented for the three aided INS architectures can be assessed using the tests discussed in Section 3. The observability test is given in equation (12). The stochastic observability test is outlined in Figure 1. The system matrices for the tests are formulated in Section 4.3. Figures 10 and 11 show the application of the observability tests for scenario A with the PVH aided INS architecture. Figures 12

and 13 show the application of the observability tests for scenario A with the PV aided INS architecture. Figure 14 shows the application of the observability tests for scenario B with the P aided INS architecture. In Figures 10 and 12, the $1 - \sigma$ estimation error bands predicted by the \bar{Q}_{k+1} term, equation (19), of the stochastic observability test are represented by solid lines whereas the $1 - \sigma$ estimation error bands computed by the EKF are represented by dashed lines.

Figure 10 shows that the stochastic system selected for scenario A and the PVH aided INS architecture is observable because the observability grammian has full rank following two measurement updates. This system is observable because the aiding system sensors directly measure the entire vehicle kinematic state independent of the vehicle maneuver. Therefore, the results of the observability test indicate that this system has met the necessary conditions to ensure the estimated state covariance matrix is bounded.

Figure 10 also shows that the EKF implemented for this stochastic system is stochastically observable because both conditions of the stochastic observability test have been satisfied. First, $\sigma_{\max}(\Lambda_{k+1}) = 0$ following two measurement updates. Therefore, sufficient information is available from the aiding sensor measurements and the vehicle maneuver so that the time evolution of P_{k+1} is independent of P_0 . Second, $\sigma_{\max}(\bar{Q}_{k+1})$ is bounded throughout the simulation time frame of 180 s. Therefore, the increases of P_{k+1} due to contributions from the matrices Q_k , Φ_k , and \bar{Q}_k are offset by decreases of P_{k+1} due to contributions from the matrices H_k , R_k , Φ_k , and \bar{Q}_k .

Figure 11 shows the effect of assuming that $\Delta_{k+1}(\alpha^{-1})$, equations (17) and (19), consists of infinitesimal components whose contributions to P_{k+1} can be neglected. The $1 - \sigma$ estimation error bands predicted by \bar{Q}_{k+1} are of the same magnitude and have the same convergence rate as the $1 - \sigma$ estimation error bands computed by the EKF. Therefore, the results of the stochastic observability test predict that the EKF implemented for scenario A and the PVH aided INS architecture will be stochastically observable. Figures 4 and 5 confirm this result.

Figure 12 shows that the stochastic system selected for scenario A and the PV aided INS architecture is observable because the observability grammian has full rank following thirteen measurement updates. This system is observable because the aiding sensors directly measure the vehicle's position and velocity vectors independent of the vehicle maneuver. Furthermore, the vehicle's angular acceleration allows the aiding sensors to indirectly measure the vehicle's heading angle. Therefore, the results of the observability

test indicate that this system has met the necessary conditions to ensure the estimated state covariance matrix is bounded.

However, Figure 12 also shows that the EKF implemented for this system is stochastically unobservable because both conditions of the stochastic observability test have not been satisfied. First, $\sigma_{\max}(\Lambda_{k+1}) = 0$ following 133 measurement updates. Therefore, sufficient information is available from the aiding sensor measurements and the vehicle maneuver so that the time evolution of P_{k+1} is independent of P_0 . But, $\sigma_{\max}(\bar{Q}_{k+1})$ is not bounded and increases throughout the simulation times of 40 s to 180 s. Therefore, the increases of P_{k+1} due to contributions from the matrices Q_k , Φ_k , and \bar{Q}_k are not offset by decreases of P_{k+1} due to contributions from the matrices H_k , R_k , Φ_k , and \bar{Q}_k .

The system is observable because the modes of the state vector are persistently excited by the vehicle's angular acceleration. However, observability does not guarantee that the estimated state covariance matrix will be bounded because the noise covariance matrices and initial state covariance matrix are not incorporated into the observability test. The stochastic observability test indicates that alternative aiding sensors, vehicle maneuvers, or process noise covariance matrix must be selected in the design of the stochastic system to bound the estimate state covariance matrix. In this case, the vehicle maneuver of scenario A was insufficient for the aiding system sensors to indirectly measure the vehicle's heading angle.

Figure 13 shows the effect of assuming that $\Delta_{k+1}(\alpha^{-1})$ consists of infinitesimal components whose contributions to P_{k+1} can be neglected. The $1 - \sigma$ estimation error bands predicted by \bar{Q}_{k+1} are of the same order of magnitude and have the same convergence rate as the $1 - \sigma$ estimation error bands computed by the EKF. Therefore, the results of the stochastic observability test predict that the EKF implemented for scenario A and the PV aided INS architecture will be stochastically unobservable. Furthermore, \bar{Q}_{k+1} identifies the modes that lead to the stochastic unobservability of a system. However, Figures 6 and 7 also show the limitations of the stochastic observability test. These figures show the estimate of the gyro null shift has a bias of $0.09^\circ/s$. The stochastic observability test can not predict a bias in the estimates of the state mean vector but can predict whether the estimated state covariance matrix is bounded. Figures 6 and 7 confirm this result.

Figure 14 shows that the stochastic system selected for scenario B and the P aided INS architecture is unobservable because the observability grammian does not have full rank. This system is unobservable because the vehicle maneuver does not allow the aiding sensors

to measure the vehicle's heading angle. Figure 14 also shows that the EKF implemented for the system is stochastically unobservable because $\sigma_{\max}(\Lambda_{k+1}) \neq 0$. Therefore, sufficient information was not available from aiding sensor measurements and the vehicle maneuver to bound the estimated state covariance matrix. The results of the stochastic observability test predict that the EKF implemented for scenario B and the P aided INS architecture will be stochastically unobservable. Figures 8 and 9 confirm this result.

5 Conclusions

In this paper, we developed a test to assess the stochastic observability of KFs implemented for discrete LTV stochastic systems consisting of known, deterministic time-varying parameters. We refer to stochastic observability as convergence of the state covariance matrix to within a user specified bound. We note, however, that there is no standard definition of stochastic observability. In [28], the concept of stochastic observability is extended to that of estimability which implies that the posterior state covariance matrix is smaller than the prior state covariance matrix. In [11], the concept of stochastic observability is extended to LTV stochastic systems consisting of stochastic parameters.

The test developed in Section 3 can be used to assess stochastic observability, first, for large initial state covariance matrices, second, for the selection of the system matrices including the process noise and measurement noise covariance matrices, and, third, for the selection of a vehicle maneuver. The test requires computation of the maximum singular value of two matrices formulated from the system matrices and the Riccati equation. The dimensions of these matrices correspond to the dimensions of the state vector.

The stochastic observability test was developed based on two assumptions. First, the system matrices consist of known, deterministic time-varying parameters. The applications of this test include nonlinear systems linearized about the true state vector trajectory. Therefore, this test can be used as a tool to evaluate EKF performance for different state vector trajectories prior to real-time implementation. Second, the statistics of the initial state vector are completely uncertain. Therefore, this test provides sufficient, but not necessary, conditions for the stochastic observability of a KF implemented for a system.

We illustrated the application of the stochastic observability test using the transfer alignment of an aided INS. In this application, vehicle maneuvers are selected to make the heading angle observable. However, we selected a sensor set and vehicle maneuver

to illustrate that while the system was observable, the KF implemented for the system was stochastically unobservable. Therefore, observability is only a necessary, but not sufficient, condition for the stochastic observability of a system. We then assessed the stochastic observability of the system using the same sensor set and vehicle maneuver to demonstrate the stochastic observability test will indicate that the EKF implemented for the system is stochastically unobservable. Furthermore, the test indicated that the stochastic unobservability of the system was due to the system matrices and not the initial state covariance matrix.

The stochastic observability test has several limitations. First, the test can not be used to assess the convergence and stability of the estimated state mean vector. Therefore, the test can not predict a bias error in the estimated state mean vector. Second, the test can not be used with system matrices consisting of unknown, deterministic time-varying parameters or stochastic parameters. Therefore, the test can not be used to assess the stochastic observability of EKFs implemented for nonlinear systems linearized about the estimated state vector trajectory. Third, the test does not provide statistical conditions on how sensors, sensor locations, sensor models, system matrices, or the state vector trajectory should be selected to ensure a KF implemented for a system is stochastically observable.

Acknowledgments

This work was partially supported by NASA under Minnesota Space Grant NNG05GG39H.

References

- [1] R.E. Kalman, "New Methods in Wiener Filtering Theory," *Proceedings of the First Symposium on Engineering Applications of Random Function Theory and Probability*, J.L. Bogdanoff and F. Kozin, Eds. New York: John Wiley & Sons, Inc., 1963.
- [2] A.E. Bryson and Y.C. Ho, *Applied Optimal Control : Optimization, Estimation, and Control*. Waltham, MA: Blaisdell Publishing Company, 1969, Chapter 8.
- [3] B.D.O. Anderson and J.B. Moore, "Detectability and Stabilizability of Time-Varying Discrete-Time Linear Systems," *SIAM Journal of Control and Optimization*, Vol. 19, No. 1, Jan. 1981, pp. 20-32.
- [4] F.L. Lewis, *Optimal Estimation*. New York: John Wiley & Sons, 1986, Chapter 2.

- [5] B. Delyon, "A Note on Uniform Observability," *IEEE Transactions on Automatic Control*, Vol. 46, No. 8, Aug. 2001, pp. 1326-1327.
- [6] H.W. Sorenson, "On the Error Behavior in Linear Minimum Variance Estimation Problems," *IEEE Transactions on Automatic Control*, Vol. 12, No. 5, October 1967, pp. 557-562.
- [7] J.J. Deyst and C.F. Price, "Conditions for Asymptotic Stability of the Discrete Minimum Variance Linear Estimator," *IEEE Transactions on Automatic Control*, Vol. 13, No. 6, Dec. 1968, pp. 702-705.
- [8] J.J. Deyst, "Correction to Conditions for Asymptotic Stability of the Discrete Minimum-Variance Linear Estimator," *IEEE Transactions on Automatic Control*, Vol. 18, No. 5, Oct. 1973, pp. 562-563.
- [9] F.A. Aliev and L. Ozbek, "Evaluation of Convergence Rate in the Central Limit Theorem for the Kalman Filter," *IEEE Transactions on Automatic Control*, Vol. 44, No. 10, Oct. 1999, pp. 1905-1909.
- [10] P. Bougerol, "Kalman Filtering with Random Coefficients and Contractions," *SIAM Journal of Control and Optimization*, Vol. 31, No. 4, July 1993, pp. 942-959.
- [11] V. Solo, "Stability of the Kalman Filter with Stochastic Time-Varying Parameters," *Proceedings of the 35th IEEE Conference on Decision and Control*, Kobe, Japan, Dec. 1996, pp. 57-61.
- [12] R.R. Bitmead and B.D.O. Anderson, "Lyapunov Techniques for the Exponential Stability of Linear Difference Equations with Random Coefficients," *IEEE Transactions on Automatic Control*, Vol. 25, No. 4, Aug. 1980, pp. 782-787.
- [13] L. Ljung, "Asymptotic Behavior of the Extended Kalman Filter as a Parameter Estimator for Linear Systems," *IEEE Transactions on Automatic Control*, Vol. 24, No. 1, Feb. 1979, pp. 36- 50.
- [14] L. Guo, "Estimating Time-Varying Parameters by the Kalman Filter Based Algorithm: Stability and Convergence," *IEEE Transactions on Automatic Control*, Vol. 35, No. 2, Feb. 1990, pp. 141-147.
- [15] M. Boutayeb, H. Rafaralahy, and M. Darouach, "Convergence Analysis of the Extended Kalman Filter Used as an Observer for Nonlinear Deterministic Discrete-Time Systems," *IEEE Transactions on Automatic Control*, Vol. 42. No. 4, April 1997, pp. 581-586.

- [16] T.L. Song and J.L. Speyer, "A Stochastic Analysis of a Modified Gain Extended Kalman Filter with Applications to Estimation with Bearings Only Measurements," *IEEE Transactions on Automatic Control*, Vol. 30, No. 10, Oct. 1985, pp. 940-949.
- [17] K. Reif, S. Gunther, E. Yaz, and R. Unbehauen, "Stochastic Stability of the Continuous-Time Extended Kalman Filter," *IEE Proceedings - Control Theory Applications*, Vol. 147, No. 1, Jan. 2000, pp. 45-52.
- [18] K. Reif, S. Gunther, E. Yaz, and R. Unbehauen, "Stochastic Stability of the Discrete-Time Extended Kalman Filter," *IEEE Transactions on Automatic Control*, Vol. 44, No. 4, April 1999, pp. 714-728.
- [19] B.D.O. Anderson and J.B. Moore, *Optimal Filtering*. Mineola, NY: Dover Publications, Inc. 1995, Chapter 3.
- [20] R.F. Stengel, *Optimal Control and Estimation*. Mineola, NY: Dover Publications, Inc., 1994, Chapters 2 and 4.
- [21] H.F. Chen, *Recursive Estimation and Control for Stochastic Systems*. New York: John Wiley and Sons, 1985, pp. 237.
- [22] A. Ben-Israel and T.N.E. Greville, *Generalized Inverses : Theory and Applications*, 2^{ed}. New York: Springer-Verlag, 2003, Chapter 1.
- [23] I.Y. Bar-Itzhack and N. Berman, "Control Theoretic Approach to Inertial Navigation Systems," *AIAA Journal of Guidance, Control, and, Dynamics*, Vol. 11, No. 3, May-June 1988, pp. 237-245.
- [24] D. Goshen-Meskin and I.Y. Bar-Itzhack, "Observability Analysis of Piece-Wise Constant Systems - Part I: Theory," *IEEE Transactions on Aerospace and Electronic Systems*, Vol. 28, No. 4, Oct. 1992, pp. 1056-1067.
- [25] D. Goshen-Meskin and I.Y. Bar-Itzhack, "Observability Analysis of Piece-Wise Constant Systems - Part II: Application to Inertial Navigation In-Flight Alignment," *IEEE Transactions on Aerospace and Electronic Systems*, Vol. 28, No. 4, Oct. 1992, pp. 1068-1075.
- [26] I. Rhee, M.F. Abdel-Hafez, and J.L. Speyer, "Observability of an Integrated GPS/INS During Maneuvers," *IEEE Transactions on Aerospace and Electronic Systems*, Vol. 40, No. 2, April 2004, pp. 526-535.
- [27] D. Gebre-Egziabher, R.C. Hayward, and J.D. Powell, "Design of Multi-Sensor Attitude Determination Systems," *IEEE Transactions on Aerospace and Electronic Systems*, Vol. 40, No. 2, April 2004, pp. 627-649.

- [28] Y. Baram and T. Kailath, “Estimability and Regulability of Linear Systems,” *IEEE Transactions on Automatic Control*, Vol. 33, No. 12, Dec. 1988, pp. 1116-1121.
- [29] V.L. Bageshwar, *Quantifying Performance Limitations of Kalman Filters in State Vector Estimation Problems*. Ph.D. Thesis, Department of Aerospace Engineering and Mechanics, University of Minnesota, 2008, Appendix B.

Appendix A

The objective of Appendix A is to prove Lemmas 1 and 2. This appendix is organized as follows. In Section A.1, we prove three supporting Lemmas that are required in the proof of Lemmas 1 and 2. In Section A.2, we prove Lemma 1. In Section A.3, we prove Lemma 2.

A.1 Supporting Lemmas

We first make four assumptions without loss of generality and review the inverses of a block matrix and a matrix series expansion.

Assumption A.1: $\Theta \in \mathcal{M}_r^{n \times p}$

Assumption A.2: Θ has the singular value decomposition

$$\Theta = U\Sigma V^T \tag{A.1}$$

where U and V refer to $n \times n$ and $p \times p$ unitary matrices, respectively,

$$\begin{aligned} U^T U &= U U^T = I_n \\ V^T V &= V V^T = I_p, \end{aligned}$$

Σ refers to a $n \times p$ matrix with rank r

$$\Sigma = \begin{bmatrix} \Sigma_r & 0_{r \times p-r} \\ 0_{n-r \times r} & 0_{n-r \times p-r} \end{bmatrix},$$

and Σ_r refers to a full rank, $r \times r$ matrix with the singular values of Θ along its diagonal.

Assumption A.3: The symmetric matrix $M(\alpha^{-1}) \in \mathcal{M}_r^{p \times p}$ is analytic at $\alpha = \infty$ and has the following series expansion with constant term equal to the identity matrix

$$M(\alpha^{-1}) = \begin{bmatrix} X & Y \\ Y^T & Z \end{bmatrix} = I + \sum_{i=1}^{\infty} \alpha^{-i} M_i \tag{A.2}$$

where

$$\begin{aligned}
M_i &= \begin{bmatrix} X_i & Y_i \\ Y_i^T & Z_i \end{bmatrix} \\
X &= I + \sum_{i=1}^{\infty} \alpha^{-i} X_i & X \in \mathcal{M}^{r \times r} \\
Y &= \sum_{i=1}^{\infty} \alpha^{-i} Y_i & Y \in \mathcal{M}^{r \times p-r} \\
Z &= I + \sum_{i=1}^{\infty} \alpha^{-i} Z_i & Z \in \mathcal{M}_{p-r}^{p-r \times p-r}
\end{aligned}$$

Assumption A.4: The symmetric matrix $\hat{M}(\alpha^{-1}) \in \mathcal{M}_r^{p \times p}$ is analytic at $\alpha = \infty$ and has the following series expansion with constant term equal to the identity matrix

$$\hat{M}(\alpha^{-1}) = V^{-1} M V = \begin{bmatrix} \hat{X} & \hat{Y} \\ \hat{Y}^T & \hat{Z} \end{bmatrix} = I + \sum_{i=1}^{\infty} \alpha^{-i} \hat{M}_i \quad (\text{A.3})$$

where

$$\begin{aligned}
\hat{M}_i &= \begin{bmatrix} \hat{X}_i & \hat{Y}_i \\ \hat{Y}_i^T & \hat{Z}_i \end{bmatrix} \\
\hat{X} &= I + \sum_{i=1}^{\infty} \alpha^{-i} \hat{X}_i & \hat{X} \in \mathcal{M}^{r \times r} \\
\hat{Y} &= \sum_{i=1}^{\infty} \alpha^{-i} \hat{Y}_i & \hat{Y} \in \mathcal{M}^{r \times p-r} \\
\hat{Z} &= I + \sum_{i=1}^{\infty} \alpha^{-i} \hat{Z}_i & \hat{Z} \in \mathcal{M}_{p-r}^{p-r \times p-r}
\end{aligned}$$

A.1.1 Block Matrix Inversion

Consider $A \in \mathcal{M}^{m \times m}$ where

$$A = \begin{bmatrix} A_{11} & A_{12} \\ A_{21} & A_{22} \end{bmatrix} \quad (\text{A.4})$$

and where A_{11} , A_{12} , A_{21} , and A_{22} are matrices of compatible dimension. The inverse of A can be written as [20]

$$D_{11} = A_{11} - A_{12} A_{22}^{-1} A_{21} \quad (\text{A.5})$$

$$A^{-1} = \begin{bmatrix} D_{11}^{-1} & -D_{11}^{-1} A_{12} A_{22}^{-1} \\ -A_{22}^{-1} A_{21} D_{11}^{-1} & A_{22}^{-1} + A_{22}^{-1} A_{21} D_{11}^{-1} A_{12} A_{22}^{-1} \end{bmatrix} \quad (\text{A.6})$$

A.1.2 Matrix Series Inversion

Consider $A \in \mathcal{M}^{m \times m}$ with series expansion

$$A = I + \alpha^{-1}A_1 + \alpha^{-2}A_2 + \alpha^{-3}A_3 + \dots \quad (\text{A.7})$$

The inverse of A can be written as

$$A^{-1} = I + \alpha^{-1}\hat{A}_1 + \alpha^{-2}\hat{A}_2 + \alpha^{-3}\hat{A}_3 + \dots \quad (\text{A.8})$$

where $\hat{A}_1 = -A_1$, $\hat{A}_2 = A_1^2 - A_2$, and $\hat{A}_3 = -A_1^3 + A_1A_2 + A_2A_1 - A_3$.

A.1.3 Supporting Lemmas

Lemma A.1: Given the matrices Θ , M , and \hat{M} as defined in Assumptions A.1-A.4, then

$$(\alpha^{-1}M + \Theta^T\Theta)^{-1} = \alpha\Pi_{\mathcal{N}(\Theta)} + V\Xi_0V^T + \alpha^{-1}V\Xi_1V^T + \alpha^{-2}V\Xi_2V^T + \dots \quad (\text{A.9})$$

where

$$\begin{aligned} \Xi_0 &= \begin{bmatrix} \Sigma_r^{-2} & 0 \\ 0 & -\hat{Z}_1 \end{bmatrix} \\ \Xi_1 &= \begin{bmatrix} -\Sigma_r^{-4} & -\Sigma_r^{-2}\hat{Y}_1 \\ -\hat{Y}_1^T\Sigma_r^{-2} & \hat{Z}_1^2 - \hat{Z}_2 \end{bmatrix} \\ \Xi_2 &= \begin{bmatrix} \xi_{11} & \xi_{12} \\ \xi_{21} & \xi_{22} \end{bmatrix} \\ \xi_{11} &= \Sigma_r^{-2}(\Sigma_r^{-4} - \hat{X}_1\Sigma_r^{-2}) \\ \xi_{12} &= -\Sigma_r^{-2}\hat{Y}_2 + \Sigma_r^{-2}\hat{Y}_1\hat{Z}_1 + \Sigma_r^{-4}\hat{Y}_1 \\ \xi_{21} &= -\hat{Y}_2^T\Sigma_r^{-2} + \hat{Z}_1\hat{Y}_1^T\Sigma_r^{-2} + \hat{Y}_1^T\Sigma_r^{-4} \\ \xi_{22} &= -\hat{Z}_1^3 + \hat{Z}_1\hat{Z}_2 + \hat{Z}_2\hat{Z}_1 - \hat{Z}_3 + \hat{Y}_1^T\Sigma_r^{-2}\hat{Y}_1 \end{aligned}$$

Proof: If we rewrite Θ using its singular value decomposition, then

$$(\alpha^{-1}M + \Theta^T\Theta)^{-1} = V(\alpha^{-1}\hat{M} + \Sigma^T\Sigma)^{-1}V^{-1} \quad (\text{A.10})$$

If we rewrite \hat{M} using Assumption A.4, then

$$(\alpha^{-1}M + \Theta^T\Theta)^{-1} = V \begin{bmatrix} \alpha^{-1}\hat{X} + \Sigma_r^2 & \alpha^{-1}\hat{Y} \\ \alpha^{-1}\hat{Y}^T & \alpha^{-1}\hat{Z} \end{bmatrix}^{-1} V^{-1} \quad (\text{A.11})$$

The inverse term of equation (A.11) can be computed using the matrix inversion lemma given in equations (A.4)-(A.6). If we compare equation (A.11) to equations (A.4) and (A.5), then

$$A_{11} = \alpha^{-1} \hat{X} + \Sigma_r^2 \quad (\text{A.12a})$$

$$A_{12} = \alpha^{-1} \hat{Y} \quad (\text{A.12b})$$

$$A_{21} = \alpha^{-1} \hat{Y}^T \quad (\text{A.12c})$$

$$A_{22} = \alpha^{-1} \hat{Z} \quad (\text{A.12d})$$

$$D_{11} = \Sigma_r^2 + \alpha^{-1} (\hat{X} - \hat{Y} \hat{Z}^{-1} \hat{Y}^T) \quad (\text{A.12e})$$

In equation (A.12e), if we rewrite \hat{Z}^{-1} using equation (A.8), then the series expansion of $\hat{X} - \hat{Y} \hat{Z}^{-1} \hat{Y}^T$ can be written as

$$\begin{aligned} \hat{X} - \hat{Y} \hat{Z}^{-1} \hat{Y}^T &= I + \alpha^{-1} \hat{X}_1 + \alpha^{-2} (\hat{X}_2 - \hat{Y}_1 \hat{Y}_1^T) \\ &\quad + \alpha^{-3} (\hat{X}_3 - \hat{Y}_1 \hat{Y}_2^T - \hat{Y}_2 \hat{Y}_1^T + \hat{Y}_1 \hat{Z}_1 \hat{Y}_1^T) + \dots \end{aligned} \quad (\text{A.13})$$

If we substitute equations (A.12) and (A.13) into equation (A.6), then equation (A.11) can be rewritten as

$$\begin{aligned} (\alpha^{-1} M + \Theta^T \Theta)^{-1} &= \alpha V \begin{bmatrix} 0 & 0 \\ 0 & I \end{bmatrix} V^{-1} + V \Xi_0 V^{-1} + \alpha^{-1} V \Xi_1 V^{-1} \\ &\quad + \alpha^{-2} V \Xi_2 V^{-1} + \dots \end{aligned} \quad (\text{A.14})$$

where Ξ_0 , Ξ_1 , and Ξ_2 are defined in equation (A.9). The intermediate steps of this proof are given in [29, pp. 169-172].

Lemma A.2: Given the matrices Θ , M , and \hat{M} as defined in Assumptions A.1-A.4, then

$$(\alpha^{-1} M + \Theta^T \Theta)^{-1} \Theta^T = (\Theta^T \Theta)^\dagger \Theta^T + \alpha^{-1} V \Xi_1 \Sigma^T U^T + \alpha^{-2} V \Xi_2 \Sigma^T U^T + \dots \quad (\text{A.15})$$

where Ξ_1 and Ξ_2 are defined in equation (A.9).

Proof: If we rewrite Θ using its singular value decomposition and appeal to Lemma A.1, then

$$\begin{aligned} (\alpha^{-1} M + \Theta^T \Theta)^{-1} \Theta^T &= \alpha V \begin{bmatrix} 0 & 0 \\ 0 & I \end{bmatrix} \Sigma^T U^T + V \Xi_0 \Sigma^T U^T \\ &\quad + \alpha^{-1} V \Xi_1 \Sigma^T U^T + \alpha^{-2} V \Xi_2 \Sigma^T U^T + \dots \\ &= V \begin{bmatrix} (\Sigma_r^{-2}) \Sigma_r & 0 \\ 0 & 0 \end{bmatrix} U^T + \alpha^{-1} V \Xi_1 \Sigma^T U^T \\ &\quad + \alpha^{-2} V \Xi_2 \Sigma^T U^T + \dots \end{aligned} \quad (\text{A.16})$$

where Ξ_0 is defined in equation (A.9).

Lemma A.3: Given the matrices Θ , M , and \hat{M} as defined in Assumptions A.1-A.4, then

$$\Theta(\alpha^{-1}M + \Theta^T\Theta)^{-1}\Theta^T = \Theta(\Theta^T\Theta)^\dagger\Theta^T - \alpha^{-1}\Theta((\Theta^T\Theta)^\dagger)^2\Theta^T + \alpha^{-2}U\Sigma\Xi_2\Sigma^TU^T + \dots \quad (\text{A.17})$$

where Ξ_1 and Ξ_2 are defined in equation (A.9).

Proof: If we rewrite Θ using its singular value decomposition and appeal to Lemma A.1, then

$$\begin{aligned} \Theta(\alpha^{-1}M + \Theta^T\Theta)^{-1}\Theta^T &= \alpha U\Sigma \begin{bmatrix} 0 & 0 \\ 0 & I \end{bmatrix} \Sigma^TU^T + U\Sigma\Xi_0\Sigma^TU^T \\ &\quad + \alpha^{-1}U\Sigma\Xi_1\Sigma^TU^T + \alpha^{-2}U\Sigma\Xi_2\Sigma^TU^T + \dots \\ &= U \begin{bmatrix} \Sigma_r(\Sigma_r^{-2})\Sigma_r & 0 \\ 0 & 0 \end{bmatrix} U^T \\ &\quad + \alpha^{-1}U \begin{bmatrix} -\Sigma_r(\Sigma_r^{-4})\Sigma_r & 0 \\ 0 & 0 \end{bmatrix} U^T \\ &\quad + \alpha^{-2}U\Sigma\Xi_2\Sigma^TU^T + \dots \end{aligned} \quad (\text{A.18})$$

A.2 Lemma 1: Proof

Consider the time-varying Riccati equation

$$P_{k+1} = \Phi_k P_k \Phi_k^T + \Gamma_k Q_k \Gamma_k^T - \Phi_k P_k H_k^T (R_k + H_k P_k H_k^T)^{-1} H_k P_k \Phi_k^T \quad (\text{A.19})$$

where the matrices of equation (A.19) are defined in Section 2.

Let the initial state covariance matrix be diagonal with equal uncertainty for all states of the state mean vector

$$P_0 = \alpha I \quad \alpha \in \Re, \alpha > 0 \quad (\text{A.20})$$

If equation (A.20) is substituted into equation (A.19), then P_1 can be written as

$$P_1 = \alpha \Phi_0 \Phi_0^T + \Gamma_0 Q_0 \Gamma_0^T - \alpha \Phi_0 H_0^T (\alpha^{-1} R_0 + H_0 H_0^T)^{-1} H_0 \Phi_0^T \quad (\text{A.21})$$

If we define

$$M_0 = I \quad (\text{A.22})$$

$$\Theta_0 = H_0^T \Upsilon_0^{-1} \quad (\text{A.23})$$

$$\Upsilon_0^T \Upsilon_0 = R_0 \quad (\text{A.24})$$

where $\Upsilon_0 = R_0^{1/2}$, then P_1 can be rewritten as

$$P_1 = \alpha \Phi_0 \Phi_0^T + \Gamma_0 Q_0 \Gamma_0^T - \alpha \Phi_0 \Theta_0 (\alpha^{-1} M_0 + \Theta_0^T \Theta_0)^{-1} \Theta_0^T \Phi_0^T \quad (\text{A.25})$$

If we appeal to Lemma A.3 and note that M_0 is not a function of α , then P_1 can be rewritten as

$$\begin{aligned} P_1 &= \alpha \Phi_0 [I - \Theta_0 (\Theta_0^T \Theta_0)^\dagger \Theta_0^T] \Phi_0^T \\ &\quad + \Gamma_0 Q_0 \Gamma_0^T + \Phi_0 \Theta_0 ((\Theta_0^T \Theta_0)^\dagger)^2 \Theta_0^T \Phi_0^T \\ &\quad - \Phi_0 [\alpha^{-1} \Theta_0 ((\Theta_0^T \Theta_0)^\dagger)^4 \Theta_0^T + \dots] \Phi_0^T \end{aligned} \quad (\text{A.26})$$

In equation (A.26), the term $\Theta_0 (\Theta_0^T \Theta_0)^\dagger \Theta_0^T$ is the projector of a vector onto the range space of Θ_0 whereas the term $I - \Theta_0 (\Theta_0^T \Theta_0)^\dagger \Theta_0^T$ is the projector of a vector onto the orthogonal complement of the range space of Θ_0

$$\Theta_0 (\Theta_0^T \Theta_0)^\dagger \Theta_0^T = \Pi_{\mathcal{R}(\Theta_0)} \quad (\text{A.27a})$$

$$I - \Theta_0 (\Theta_0^T \Theta_0)^\dagger \Theta_0^T = \Pi_{\mathcal{N}(\Theta_0^T)} \quad (\text{A.27b})$$

If equation (A.27) is substituted into equation (A.26), then P_1 can be rewritten as

$$P_1 = \alpha \Lambda_1 + \bar{Q}_1 + \Delta_1(\alpha^{-1}) \quad (\text{A.28})$$

where

$$\Pi_{\mathcal{N}(\Theta_0^T)} = \Omega_0 \Omega_0^T \quad (\text{A.28a})$$

$$\Lambda_1 = \Phi_0 \Omega_0 \Omega_0^T \Phi_0^T \quad (\text{A.28b})$$

$$\bar{Q}_1 = \Gamma_0 Q_0 \Gamma_0^T + \Phi_0 \Theta_0 ((\Theta_0^T \Theta_0)^\dagger)^2 \Theta_0^T \Phi_0^T \quad (\text{A.28c})$$

$$\Delta_1(\alpha^{-1}) = -\Phi_0 [\alpha^{-1} \Theta_0 ((\Theta_0^T \Theta_0)^\dagger)^4 \Theta_0^T + \dots] \Phi_0^T \quad (\text{A.28d})$$

and where Ω_0 has the same rank as $\Pi_{\mathcal{N}(\Theta_0^T)}$. The intermediate steps in the derivation of P_1 are given in [29, pp. 174-176].

Equation (A.28) suggests that the general form of P_k is

$$P_k = \alpha \Lambda_k + \bar{Q}_k + \Delta_k(\alpha^{-1}) \quad (\text{A.29})$$

If equation (A.29) is substituted into equation (A.19), then P_{k+1} can be rewritten as

$$\begin{aligned} P_{k+1} &= \alpha \Phi_{k,0} \Omega_{0,k-1} \Omega_{0,k-1}^T \Phi_{k,0}^T + \Phi_k \bar{Q}_k \Phi_k^T + \Gamma_k Q_k \Gamma_k^T + \Phi_k \Delta_k \Phi_k^T \\ &\quad - \Phi_k (\alpha \Phi_{k-1,0} \Omega_{0,k-1} \Omega_{0,k-1}^T \Phi_{k-1,0}^T + \bar{Q}_k + \Delta_k) H_k^T \times \\ &\quad \times [R_k + H_k \bar{Q}_k H_k^T + H_k \Delta_k H_k^T + \alpha H_k \Phi_{k-1,0} \Omega_{0,k-1} \Omega_{0,k-1}^T \Phi_{k-1,0}^T H_k^T]^{-1} \times \\ &\quad \times H_k (\alpha \Phi_{k-1,0} \Omega_{0,k-1} \Omega_{0,k-1}^T \Phi_{k-1,0}^T + \bar{Q}_k + \Delta_k) \Phi_k^T \end{aligned} \quad (\text{A.30})$$

The terms of equation (A.30) can now be expanded so that the α terms can be identified and collected. If we define

$$M_k = I + \Upsilon_k^{-T} H_k \Delta_k H_k^T \Upsilon_k^{-1} \quad (\text{A.31})$$

$$\Theta_k = \Omega_{0,k-1}^T \Phi_{k-1,0}^T H_k^T \Upsilon_k^{-1} \quad (\text{A.32})$$

$$\Upsilon_k^T \Upsilon_k = R_k + H_k \bar{Q}_k H_k^T \quad (\text{A.33})$$

where $\Upsilon_k = (R_k + H_k \bar{Q}_k H_k^T)^{1/2}$ and we appeal to Lemmas A.1-A.3, then P_{k+1} can be written as

$$\begin{aligned} P_{k+1} &= \alpha \Phi_{k,0} \Omega_{0,k-1} \Omega_{0,k-1}^T \Phi_{k,0}^T + \Phi_k \bar{Q}_k \Phi_k^T + \Gamma_k Q_k \Gamma_k^T + \Phi_k \Delta_k \Phi_k^T \\ &\quad - \Phi_{k,0} \Omega_{0,k-1} [\alpha \Theta_k (\Theta_k^T \Theta_k)^\dagger \Theta_k^T - \Theta_k ((\Theta_k^T \Theta_k)^\dagger)^2 \Theta_k^T] \Omega_{0,k-1}^T \Phi_{k,0}^T \\ &\quad - \Phi_{k,0} \Omega_{0,k-1} [\alpha^{-1} \Theta_k ((\Theta_k^T \Theta_k)^\dagger)^4 \Theta_k^T + \dots] \Omega_{0,k-1}^T \Phi_{k,0}^T \\ &\quad - \Phi_{k,0} \Omega_{0,k-1} [\Theta_k (\Theta_k^T \Theta_k)^\dagger + \alpha^{-1} U_k \Sigma_k \Xi_{k,1}^T V_k^T + \dots] \Upsilon_k^{-T} H_k \bar{Q}_k \Phi_k^T \\ &\quad - \Phi_{k,0} \Omega_{0,k-1} [\Theta_k (\Theta_k^T \Theta_k)^\dagger + \alpha^{-1} U_k \Sigma_k \Xi_{k,1}^T V_k^T + \dots] \Upsilon_k^{-T} H_k \Delta_k \Phi_k^T \\ &\quad - \Phi_k \bar{Q}_k H_k^T \Upsilon_k^{-1} [(\Theta_k^T \Theta_k)^\dagger \Theta_k^T + \alpha^{-1} V_k \Xi_{k,1} \Sigma_k^T U_k^T + \dots] \Omega_{0,k-1}^T \Phi_{k,0}^T \\ &\quad - \Phi_k \bar{Q}_k H_k^T \Upsilon_k^{-1} [\Pi_{\mathcal{N}(\Theta_k)} + \alpha^{-1} V_k \Xi_{k,0} V_k^{-1} + \dots] \Upsilon_k^{-T} H_k \bar{Q}_k \Phi_k^T \\ &\quad - \Phi_k \bar{Q}_k H_k^T \Upsilon_k^{-1} [\Pi_{\mathcal{N}(\Theta_k)} + \alpha^{-1} V_k \Xi_{k,0} V_k^{-1} + \dots] \Upsilon_k^{-T} H_k \Delta_k \Phi_k^T \\ &\quad - \Phi_k \Delta_k H_k^T \Upsilon_k^{-1} [(\Theta_k^T \Theta_k)^\dagger \Theta_k^T + \alpha^{-1} V_k \Xi_{k,1} \Sigma_k^T U_k^T + \dots] \Omega_{0,k-1}^T \Phi_{k,0}^T \\ &\quad - \Phi_k \Delta_k H_k^T \Upsilon_k^{-1} [\Pi_{\mathcal{N}(\Theta_k)} + \alpha^{-1} V_k \Xi_{k,0} V_k^{-1} + \dots] \Upsilon_k^{-T} H_k \bar{Q}_k \Phi_k^T \\ &\quad - \Phi_k \Delta_k H_k^T \Upsilon_k^{-1} [\Pi_{\mathcal{N}(\Theta_k)} + \alpha^{-1} V_k \Xi_{k,0} V_k^{-1} + \dots] \Upsilon_k^{-T} H_k \Delta_k \Phi_k^T \end{aligned} \quad (\text{A.34})$$

In equation (A.34), the term $\Theta_k(\Theta_k^T \Theta_k)^\dagger \Theta_k^T$ is the projector of a vector onto the range space of Θ_k whereas the term $I - \Theta_k(\Theta_k^T \Theta_k)^\dagger \Theta_k^T$ is the projector of a vector onto the orthogonal complement of the range space of Θ_k

$$\Theta_k(\Theta_k^T \Theta_k)^\dagger \Theta_k^T = \Pi_{\mathcal{R}(\Theta_k)} \quad (\text{A.35a})$$

$$I - \Theta_k(\Theta_k^T \Theta_k)^\dagger \Theta_k^T = \Pi_{\mathcal{N}(\Theta_k^T)} \quad (\text{A.35b})$$

If equation (A.35) is substituted into equation (A.34), then P_{k+1} can be written as

$$P_{k+1} = \alpha \Lambda_{k+1} + \bar{Q}_{k+1} + \Delta_{k+1}(\alpha^{-1}) \quad (\text{A.36})$$

where

$$\Pi_{\mathcal{N}(\Theta_k^T)} = \Omega_k \Omega_k^T \quad (\text{A.36a})$$

$$\Lambda_{k+1} = \Phi_{k,0} \Omega_{0,k} \Omega_{0,k}^T \Phi_{k,0}^T \quad (\text{A.36b})$$

$$\begin{aligned} \bar{Q}_{k+1} = & \Phi_k \bar{Q}_k \Phi_k^T + \Gamma_k Q_k \Gamma_k^T \\ & + \Phi_{k,0} \Omega_{0,k-1} \Theta_k ((\Theta_k^T \Theta_k)^\dagger)^2 \Theta_k^T \Omega_{0,k-1}^T \Phi_{k,0}^T \\ & - \Phi_{k,0} \Omega_{0,k-1} \Theta_k (\Theta_k^T \Theta_k)^\dagger \Upsilon_k^{-T} H_k \bar{Q}_k \Phi_{k,0}^T \\ & - \Phi_k \bar{Q}_k H_k^T \Upsilon_k^{-1} (\Theta_k^T \Theta_k)^\dagger \Theta_k^T \Omega_{0,k-1}^T \Phi_{k,0}^T \\ & - \Phi_k \bar{Q}_k H_k^T \Upsilon_k^{-1} \Pi_{\mathcal{N}(\Theta_k)} \Upsilon_k^{-T} H_k \bar{Q}_k \Phi_k^T \end{aligned} \quad (\text{A.36c})$$

$$\begin{aligned} \Delta_{k+1}(\alpha^{-1}) = & \Phi_k \Delta_k \Phi_k^T \\ & - \Phi_{k,0} \Omega_{0,k-1} [\alpha^{-1} \Theta_k ((\Theta_k^T \Theta_k)^\dagger)^4 \Theta_k^T + \dots] \Omega_{0,k-1}^T \Phi_{k,0}^T \\ & - \Phi_{k,0} \Omega_{0,k-1} [\alpha^{-1} U_k \Sigma_k \Xi_{k,1}^T V_k^T + \dots] \Upsilon_k^{-T} H_k \bar{Q}_k \Phi_{k,0}^T \\ & - \Phi_{k,0} \Omega_{0,k-1} [\Theta_k (\Theta_k^T \Theta_k)^\dagger + \alpha^{-1} U_k \Sigma_k \Xi_{k,1}^T V_k^T + \dots] \Upsilon_k^{-T} H_k \Delta_k \Phi_{k,0}^T \\ & - \Phi_k \bar{Q}_k H_k^T \Upsilon_k^{-1} [\alpha^{-1} V_k \Xi_{k,1} \Sigma_k^T U_k^T + \dots] \Omega_{0,k-1}^T \Phi_{k,0}^T \\ & - \Phi_k \bar{Q}_k H_k^T \Upsilon_k^{-1} [\alpha^{-1} V_k \Xi_{k,0} V_k^{-1} + \dots] \Upsilon_k^{-T} H_k \bar{Q}_k \Phi_k^T \\ & - \Phi_k \bar{Q}_k H_k^T \Upsilon_k^{-1} [\Pi_{\mathcal{N}(\Theta_k)} + \alpha^{-1} V_k \Xi_{k,0} V_k^{-1} + \dots] \Upsilon_k^{-T} H_k \Delta_k \Phi_k^T \\ & - \Phi_k \Delta_k H_k^T \Upsilon_k^{-1} [(\Theta_k^T \Theta_k)^\dagger \Theta_k^T + \alpha^{-1} V_k \Xi_{k,1} \Sigma_k^T U_k^T + \dots] \Omega_{0,k-1}^T \Phi_{k,0}^T \\ & - \Phi_k \Delta_k H_k^T \Upsilon_k^{-1} [\Pi_{\mathcal{N}(\Theta_k)} + \alpha^{-1} V_k \Xi_{k,0} V_k^{-1} + \dots] \Upsilon_k^{-T} H_k \bar{Q}_k \Phi_k^T \\ & - \Phi_k \Delta_k H_k^T \Upsilon_k^{-1} [\Pi_{\mathcal{N}(\Theta_k)} + \alpha^{-1} V_k \Xi_{k,0} V_k^{-1} + \dots] \Upsilon_k^{-T} H_k \Delta_k \Phi_k^T \end{aligned} \quad (\text{A.36d})$$

and where Ω_k has the same rank as $\Pi_{\mathcal{N}(\Theta_k^T)}$. The intermediate steps in the derivation of P_{k+1} are given in [29, pp. 184-188].

A.3 Lemma 2: Proof

If $\sigma_{\max}(\Lambda_k) = 0$, then the general form of P_k , equation (A.29), is

$$P_k = \bar{Q}_k + \Delta_k(\alpha^{-1}) \quad (\text{A.37})$$

If equation (A.37) is substituted into equation (A.19), then P_{k+1} can be rewritten as

$$\begin{aligned} P_{k+1} &= \Phi_k \bar{Q}_k \Phi_k^T + \Gamma_k Q_k \Gamma_k^T + \Phi_k \Delta_k \Phi_k^T \\ &\quad - \Phi_k (\bar{Q}_k + \Delta_k) H_k^T \times \\ &\quad \times [R_k + H_k \bar{Q}_k H_k^T + H_k \Delta_k H_k^T]^{-1} H_k (\bar{Q}_k + \Delta_k) \Phi_k^T \end{aligned} \quad (\text{A.38})$$

The terms of equation (A.38) can now be expanded so that the α terms can be identified and collected. If we define

$$M_k = I + \Upsilon_k^{-T} H_k \Delta_k H_k^T \Upsilon_k^{-1} \quad (\text{A.39})$$

$$\Upsilon_k^T \Upsilon_k = R_k + H_k \bar{Q}_k H_k^T \quad (\text{A.40})$$

where $\Upsilon_k = (R_k + H_k \bar{Q}_k H_k^T)^{1/2}$, then equation (A.38) can be written as

$$\begin{aligned} P_{k+1} &= \Phi_k \bar{Q}_k \Phi_k^T + \Gamma_k Q_k \Gamma_k^T + \Phi_k \Delta_k \Phi_k^T \\ &\quad - \Phi_k \bar{Q}_k H_k^T \Upsilon_k^{-1} M_k^{-1} \Upsilon_k^{-T} H_k \bar{Q}_k \Phi_k^T \\ &\quad - \Phi_k \bar{Q}_k H_k^T \Upsilon_k^{-1} M_k^{-1} \Upsilon_k^{-T} H_k \Delta_k \Phi_k^T \\ &\quad - \Phi_k \Delta_k H_k^T \Upsilon_k^{-1} M_k^{-1} \Upsilon_k^{-T} H_k \bar{Q}_k \Phi_k^T \\ &\quad - \Phi_k \Delta_k H_k^T \Upsilon_k^{-1} M_k^{-1} \Upsilon_k^{-T} H_k \Delta_k \Phi_k^T \end{aligned} \quad (\text{A.41})$$

If we rewrite the M^{-1} term using equation (A.8), then equation (A.41) can be rewritten as

$$P_{k+1} = \bar{Q}_{k+1} + \Delta_{k+1}(\alpha^{-1}) \quad (\text{A.42})$$

where

$$\bar{Q}_{k+1} = \Phi_k \bar{Q}_k \Phi_k^T + \Gamma_k Q_k \Gamma_k^T - \Phi_k \bar{Q}_k H_k^T \Upsilon_k^{-1} \Upsilon_k^{-T} H_k \bar{Q}_k \Phi_k^T \quad (\text{A.42a})$$

$$\begin{aligned} \Delta_{k+1}(\alpha^{-1}) &= \Phi_k \Delta_k \Phi_k^T \\ &\quad - \Phi_k \bar{Q}_k H_k^T \Upsilon_k^{-1} [-\alpha^{-1} M_{k,1} + \dots] \Upsilon_k^{-T} H_k \bar{Q}_k \Phi_k^T \\ &\quad - \Phi_k \bar{Q}_k H_k^T \Upsilon_k^{-1} [I - \alpha^{-1} M_{k,1} + \dots] \Upsilon_k^{-T} H_k \Delta_k \Phi_k^T \\ &\quad - \Phi_k \Delta_k H_k^T \Upsilon_k^{-1} [I - \alpha^{-1} M_{k,1} + \dots] \Upsilon_k^{-T} H_k \bar{Q}_k \Phi_k^T \\ &\quad - \Phi_k \Delta_k H_k^T \Upsilon_k^{-1} [I - \alpha^{-1} M_{k,1} + \dots] \Upsilon_k^{-T} H_k \Delta_k \Phi_k^T \end{aligned} \quad (\text{A.42b})$$

The intermediate steps in the derivation of P_{k+1} are given in [29, pp. 188-190].

f_{bx0}, f_{by0}	0.1g
τ_{ax}, τ_{ay}	300 s
σ_{abl_x}	0.001g
σ_{abl_y}	0.002g
σ_{ax}, σ_{ay}	0.001g
ω_{bz0}	0.5°/s
τ_g	300 s
σ_{gbl}	0.05°/s
σ_g	0.001°/s
σ_{pN}, σ_{pE}	0.1 m
σ_{vN}, σ_{vE}	0.01 m/s
σ_ψ	0.25°
g	9.81 m/s ²

Table 1: Aided INS Sensor Statistics

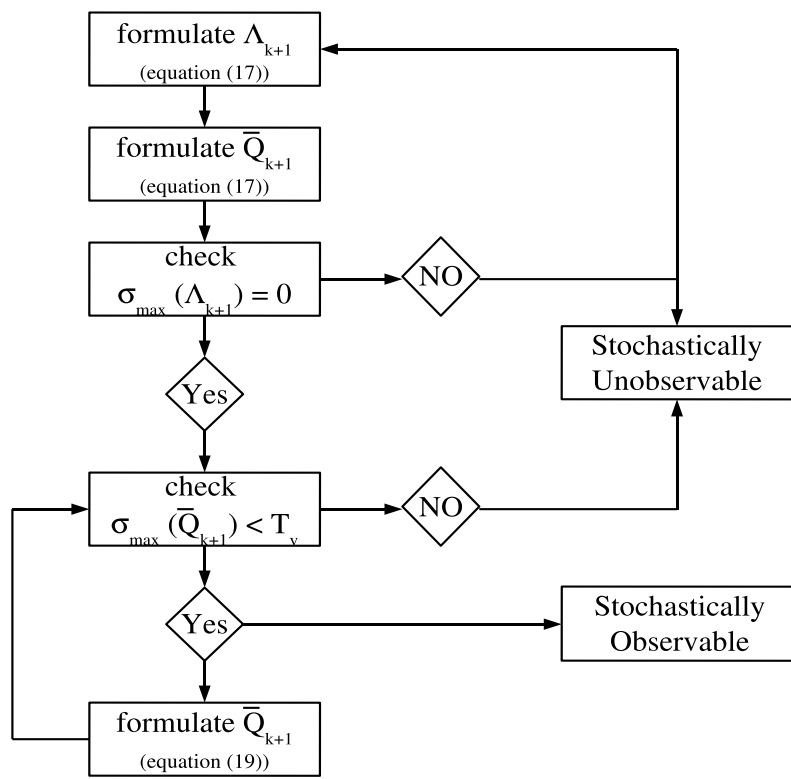


Figure 1: Stochastic Observability Test

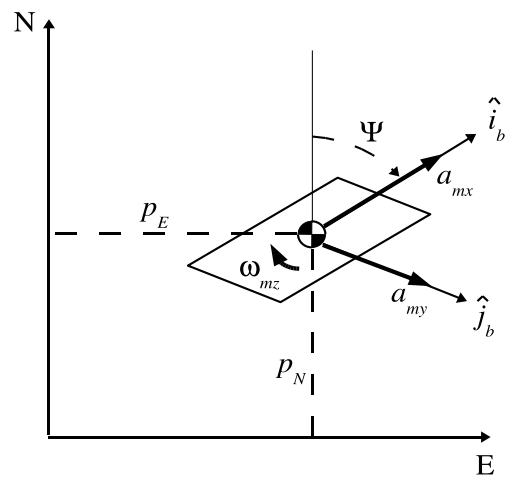


Figure 2: Vehicle Definition

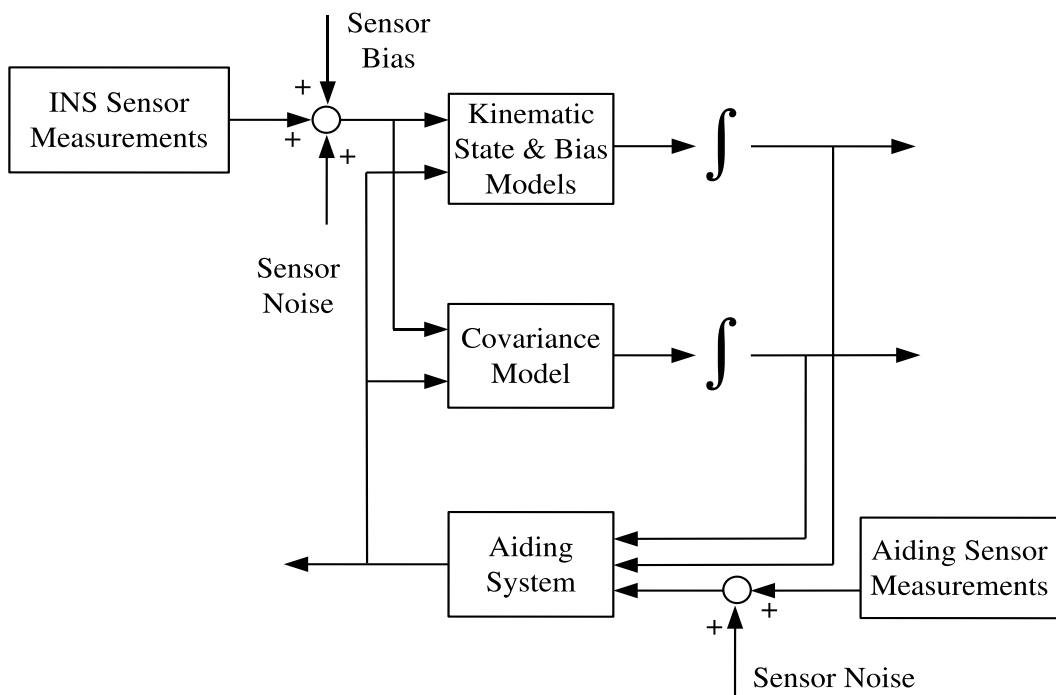


Figure 3: Aided INS Architecture

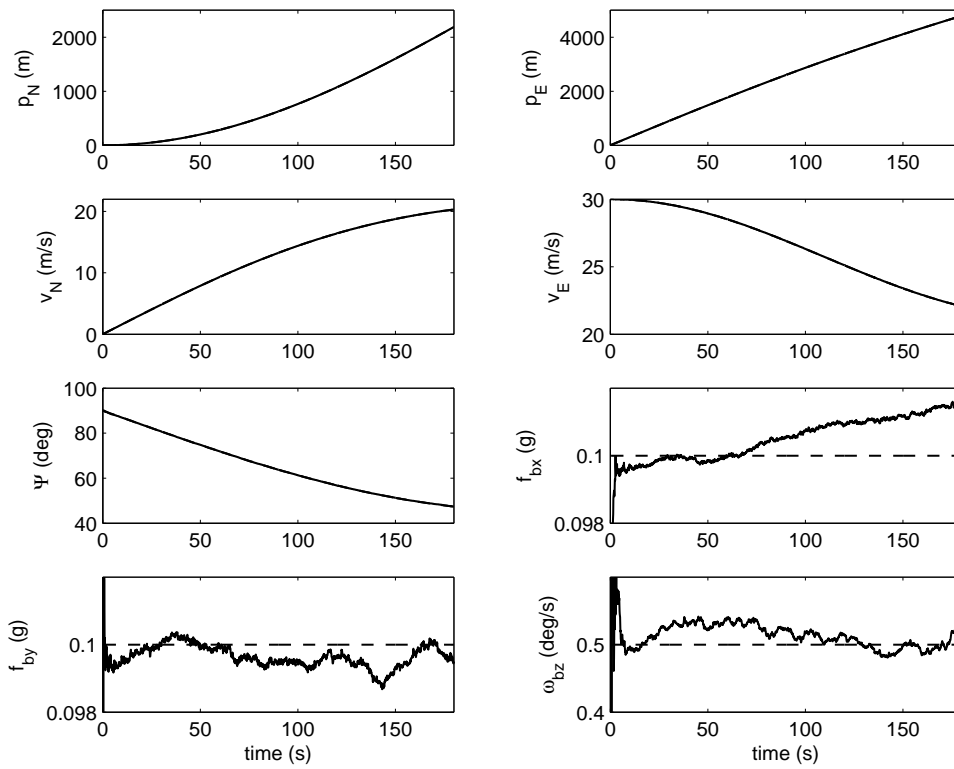


Figure 4: Estimated State Mean Vector
Scenario A; PVH Aiding System

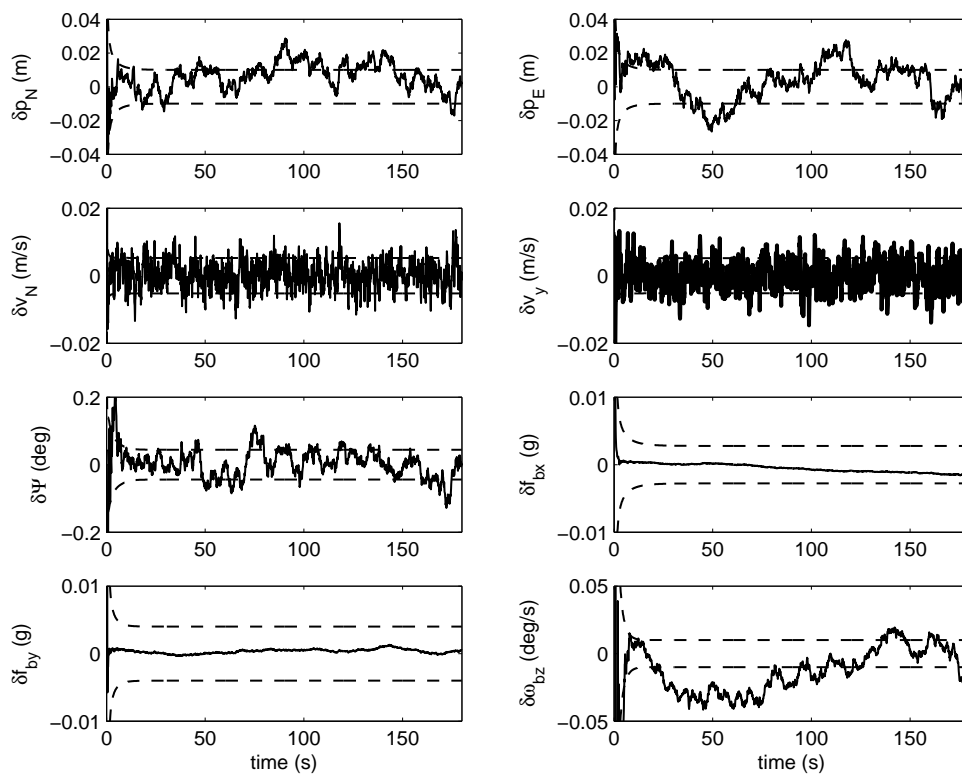


Figure 5: Estimated State Error Vector
Scenario A; PVH Aiding System

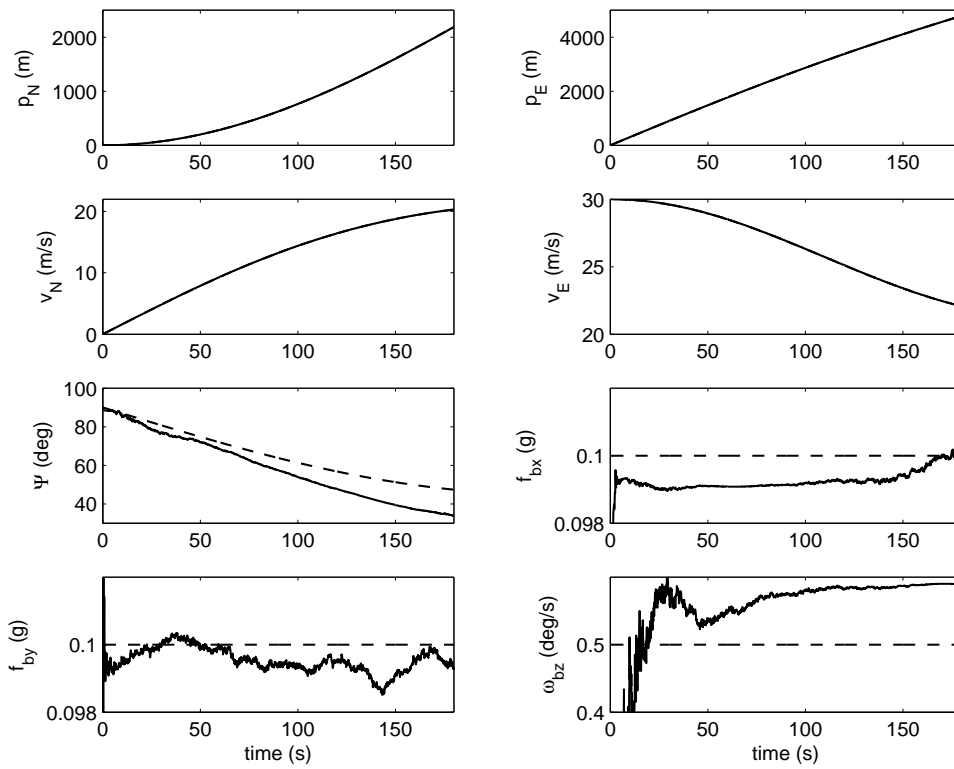


Figure 6: Estimated State Mean Vector
Scenario A; PV Aiding System

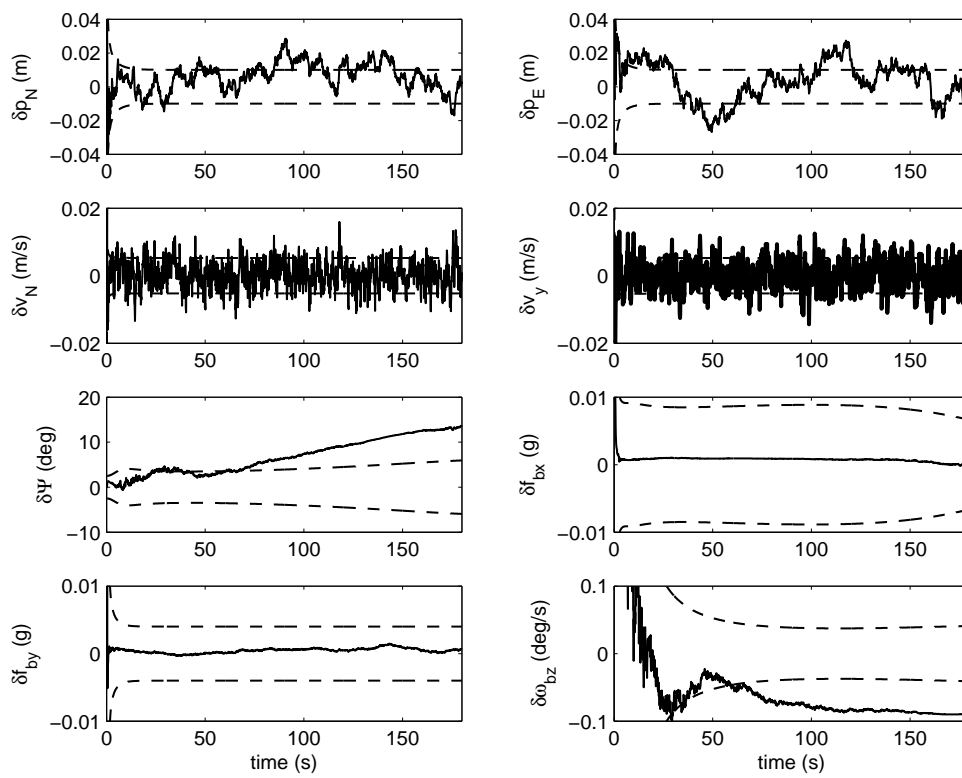


Figure 7: Estimated State Error Vector
Scenario A; PV Aiding System

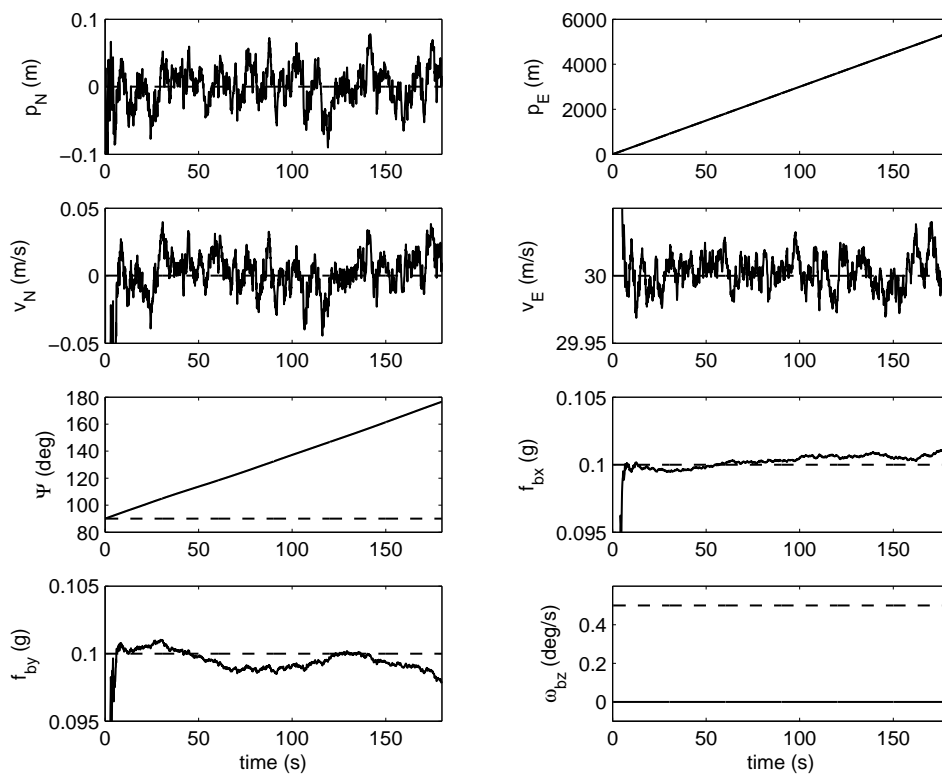


Figure 8: Estimated State Mean Vector
Scenario B; P Aiding System

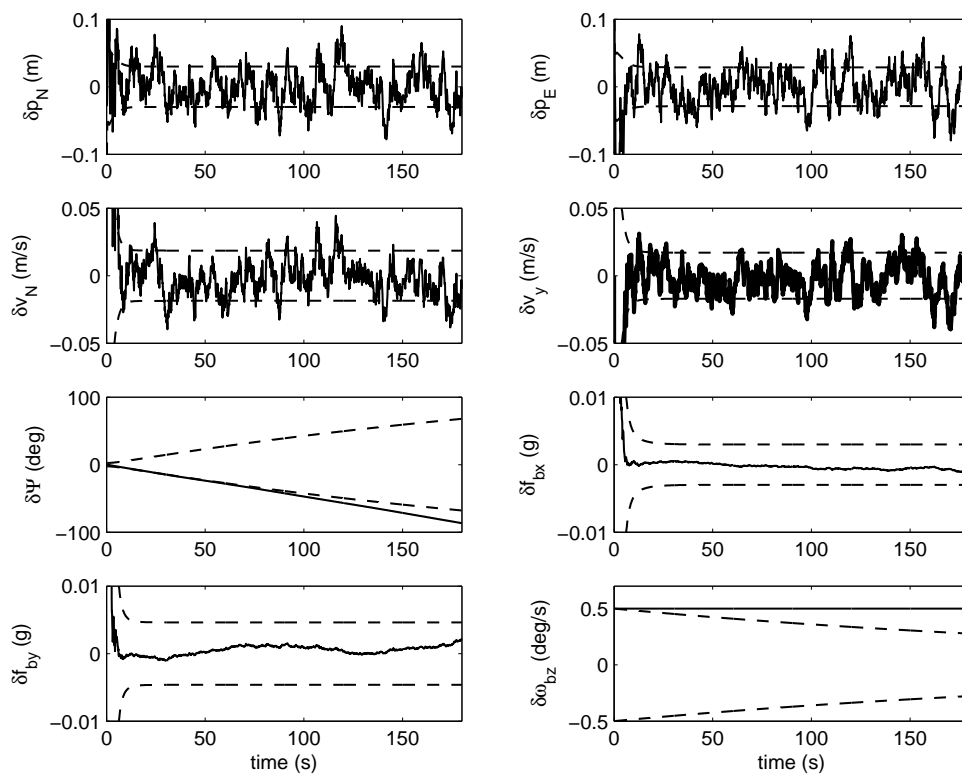


Figure 9: Estimated State Error Vector
Scenario B; P Aiding System

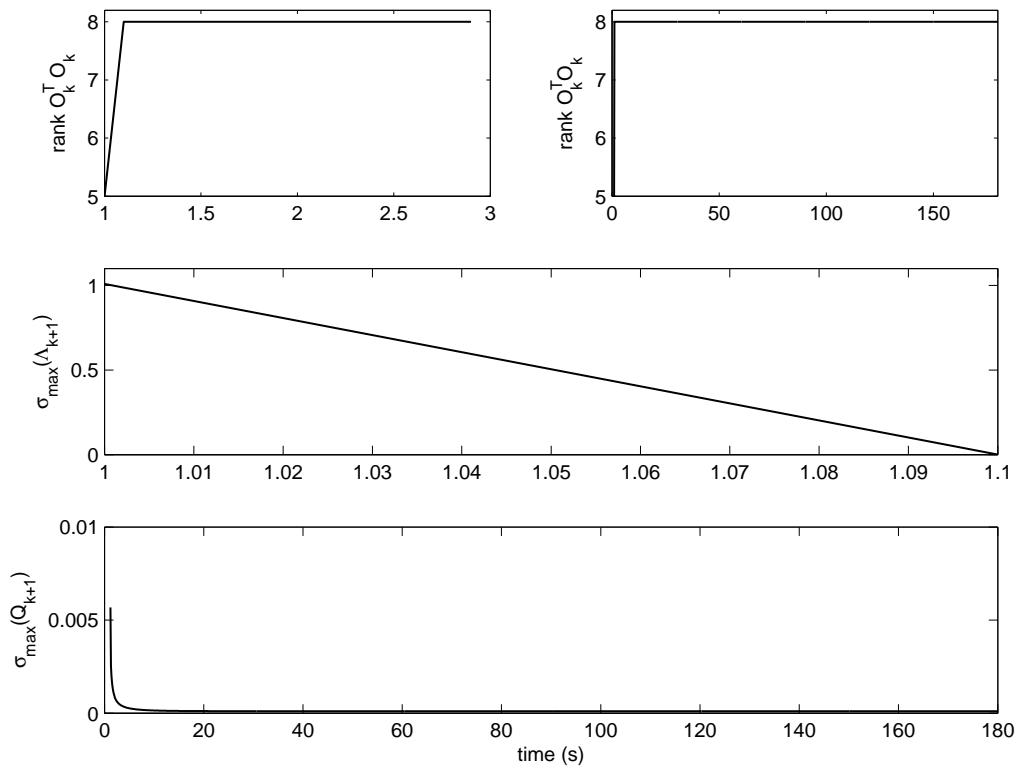


Figure 10: Observability Tests
 Scenario A; PVH Aiding System

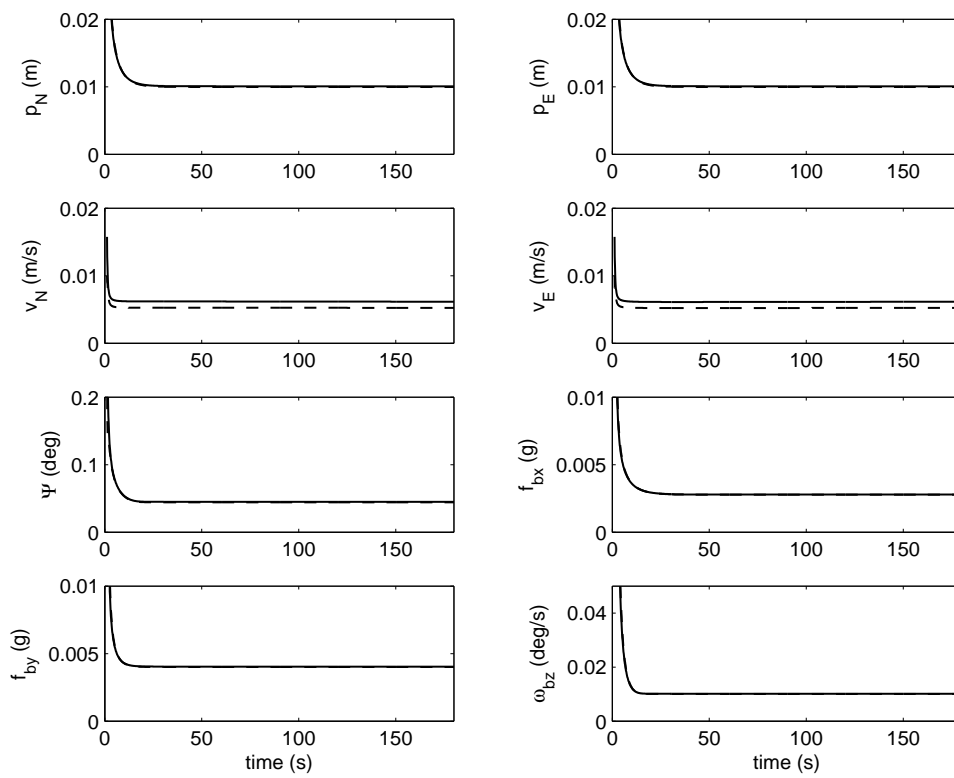


Figure 11: Comparison of Estimated Variances
Scenario A; PVH Aiding System

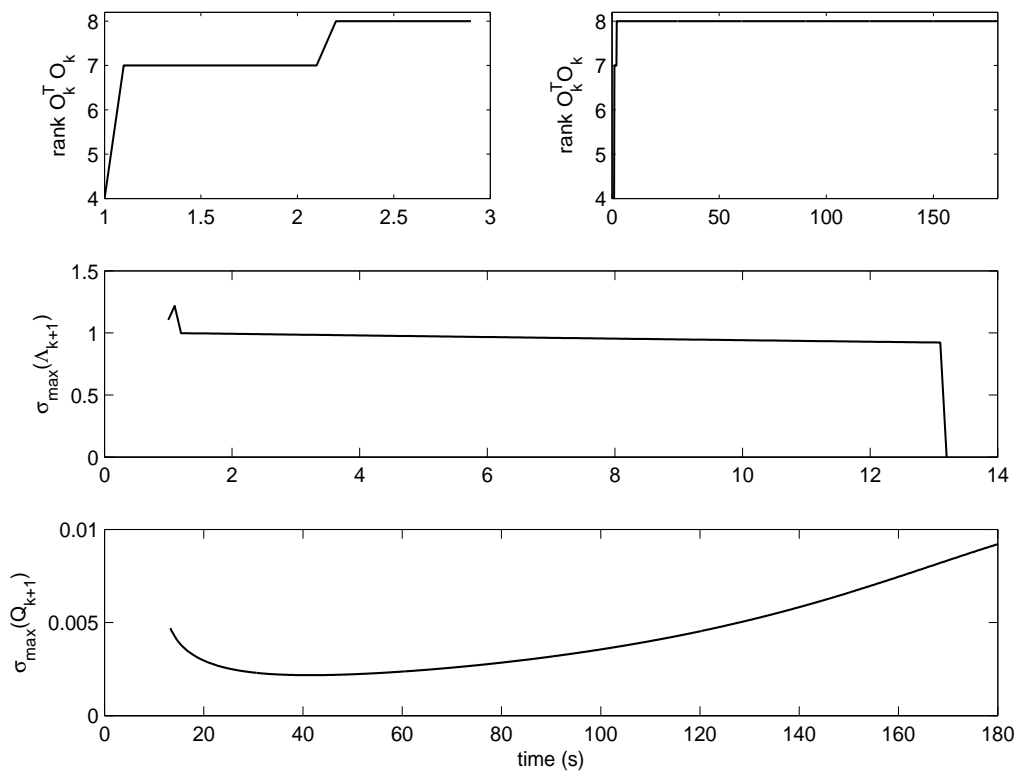


Figure 12: Observability Tests
Scenario A; PV Aiding System

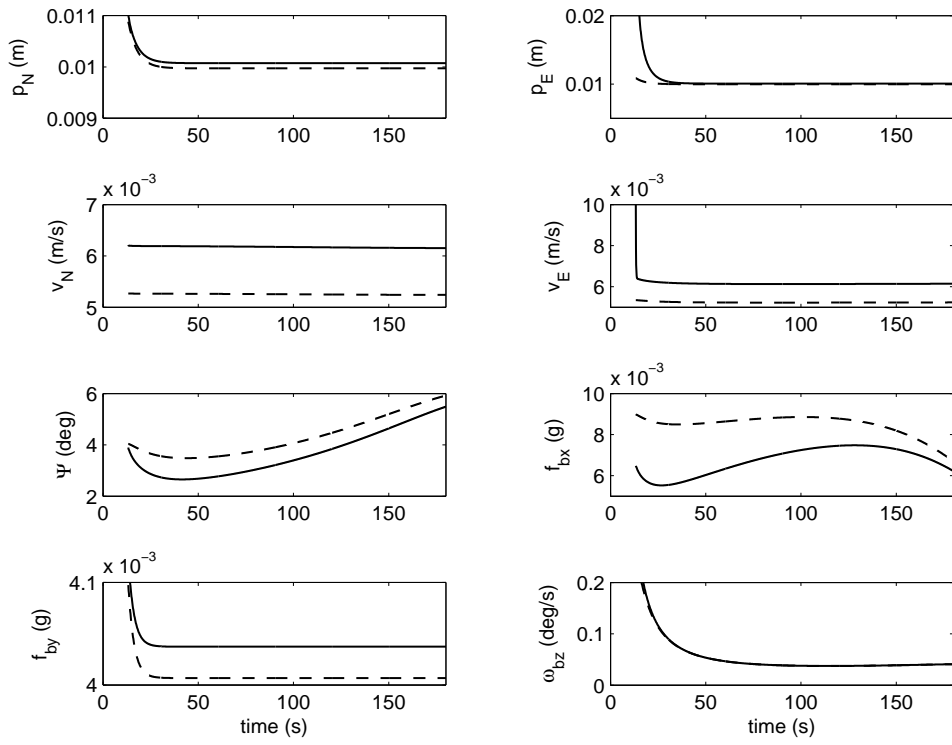


Figure 13: Comparison of Estimated Variances
Scenario A; PV Aiding System

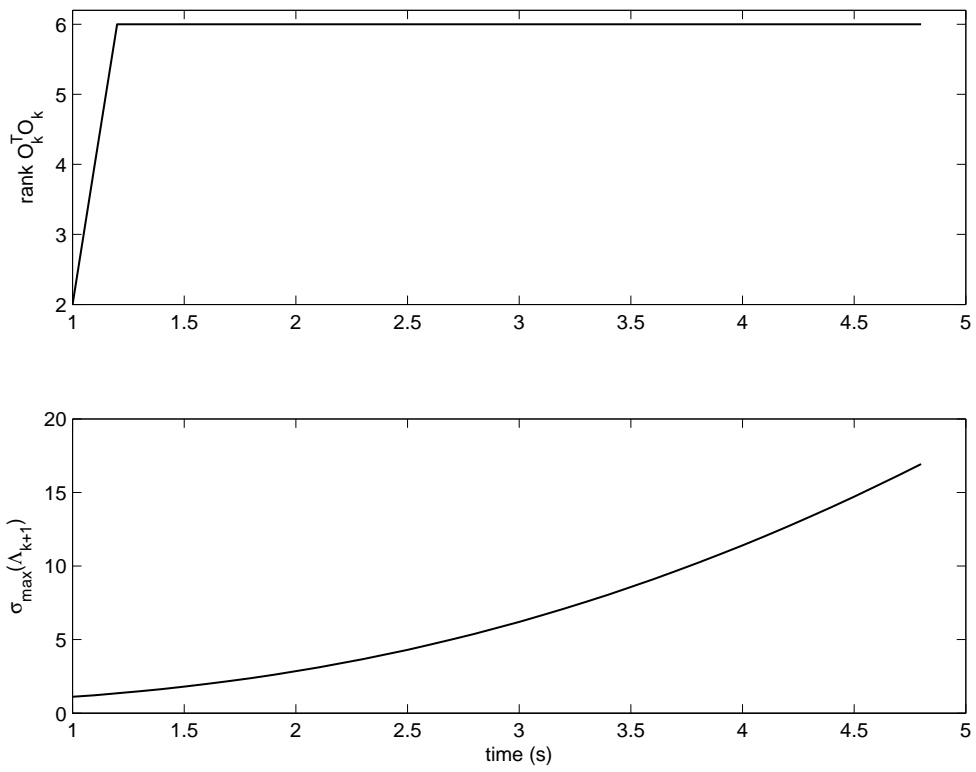


Figure 14: Observability Tests
Scenario B; P Aiding System